



REVIEW ARTICLE

Synthesis of iron-based magnetic nanocomposites: A review



Is Fatimah^a, Ganjar Fadillah^a, Septian P. Yudha^b

^a Department of Chemistry, Faculty of Mathematics and Natural Sciences, Universitas Islam Indonesia, Kampus Terpadu UII, Jl. Kaliurang Km 14, Sleman, Yogyakarta, Indonesia

^b Santo Paulus Polytechnic, Surakarta, Jl. Dr. Radjiman No.659R Pajang Laweyan Surakarta, Indonesia

Received 15 April 2021; accepted 26 June 2021

Available online 2 July 2021

KEYWORDS

Magnetic;
Magnetic nanocomposite;
Iron oxide nanoparticles

Abstract Iron oxide-based magnetic nanocomposites have been interesting materials for a wide range of applications in various fields of environment, energy, industries, and medicals. The formation of iron oxide-based magnetic nanocomposites is varied and tuneable referred to their purposes. This paper presents the reviews of the development of magnetic iron oxide nanocomposites by several synthesis method and materials. The highlight is focused on various method for controlling size, magnetization, and the nanoparticles distribution within solid support such as mesoporous silica, clay, graphene, carbon, and zeolite. The role of synthesis method on the magnetic properties and other characteristics as the function of various parameters such as iron content, synthesis condition such as pH, dispersion method, and the presence of intensification are summarized. Furthermore, future perspective for development is also highlighted.

© 2021 The Author(s). Published by Elsevier B.V. on behalf of King Saud University. This is an open access article under the CC BY-NC-ND license (<http://creativecommons.org/licenses/by-nc-nd/4.0/>).

Contents

1. Introduction	2
2. Synthesis of magnetic nanocomposites.	2
2.1. Co-precipitation method	2
2.2. Chemical vapor deposition (CVD)	4
2.3. Electrochemical synthesis.	7

E-mail address: isfatimah@uii.ac.id (I. Fatimah)

Peer review under responsibility of King Saud University.



2.4. Solvothermal method	10
2.5. Microemulsion	11
2.6. Microwave-assisted synthesis	14
3. Future perspective	17
Declaration of Competing Interest	17
Acknowledgement	17
References	17

1. Introduction

Iron oxide magnetic nanoparticles and nanocomposites are one of the promising materials in many fields' application due to its unique properties both chemical and physical. As naturally, the magnetic material can be classified into three major types, that are maghemite ($\gamma\text{-Fe}_2\text{O}_3$), magnetite (Fe_3O_4) and hematite ($\alpha\text{-Fe}_2\text{O}_3$). These classifications are useful to describe the disadvantages and advantages of the materials when they were applied in specific applications. For example, magnetite material has been commonly used in medical application for drug delivery because of the highest magnetic saturation properties than the others (almost > 250 times) (Chandra et al., 2010). Therefore, determining the basic type of magnetic material is one of the important factors when the material employed in different type application. In addition, besides magnetite types, hematite magnetic nanomaterials have been widely reported in therapy, cancer treatment, hypothermia treatment, and drug delivery systems. In other hands, the material properties such superparamagnetic, which correlated with thermal energy and the ferromagnetic nanoparticle is one of important character for sensor and biomedical purposes (Cardoso et al., 2017). The magnetic properties of iron oxide material depend on the type of the individual and synthesis pathways of magnetic material as shown in Table 1. The basic idea of magnetic nanocomposite development was that magnetic materials are a multimagnetic domain structure, and as their size is reduced to nanoscale, they have a single magnetic domain structure, and their magnetism turns to paramagnetic (Ladj et al., 2013). The change in particle size into the critical size influences the magnetic spin of the magnetic nanomaterials into the disordered and superparamagnetic (Medeiros et al., 2011; Schleich et al., 2014). The effect of particle size affected to magnetic properties already reported. The magnetic properties (M_s , M_r , and H_c) is directly influence by reducing or increasing the particle size. However, the particle size and magnetic properties have a linear correlation, for example increasing particle size will also increase magnetic intrinsic properties, including M_s , M_r and H_c (Li et al., 2017). These phenomena are useful for tumor thermotherapy. In different mechanism, magnetic nanoparticles can be served as vectors to bind biomolecules and then be separated from the biomolecules at the targeted area under the action of the magnetic field and thus used for targeted therapy or diagnosis. In the environmental applications, the nanocomposites were superior in adsorption, photocatalysis and catalysis, as well as in sensor and biosensor applications. Particularly, the easy in separation due to magnetically recoverable nano catalytic, adsorption and chemical bonding interaction are the potencies for adsorption and catalysis area. The combination of magnetic properties and such specific characters for specific purposes is basic idea for magnetic nanocomposite development (Cao et al., 2013). Moreover, the development of the high stability of iron oxide nanocomposite is still a challenging issue, especially in

biomedicine applications. Although iron salts are relatively more stable like Mohr's salts; however, in the liquid phase, the stability becomes decreasing. Therefore, increasing stability with a polymer already reported could increase the stability of iron ions. This technique has been widely developed for the synthesis process because it can produce a relatively more significant 3-fold percentage of iron ions composition (Spiridonov et al., 2018). The magnetic polymer core-shell was developed as a protein adsorbent material due to the material's hydrophobic properties (Elaïssari and Bourrel, 2001). Thermosensitive properties are the main characteristics of polymer-coated materials for biomedical applications. Furthermore, surface modification with polymer cation (polycation) is also widely developed and reported as absorbing and detecting viruses because it can increase the adsorption power of the material through electrostatic mechanisms (Veyret et al., 2005).

The properties and structure of combining material influence the procedure and route and synthesis method. This review highlights the synthesis of magnetic nanocomposite. Considering that the specific surface area, particle size and magnetic saturation are the important physicochemical characters, the studies focused on these parameters. In fact, the relationship among parameters affects to the properties of nanocomposite. For example, from the synthesis of magnetic iron oxide nanocomposite using clay materials, following factors significantly influence the properties of magnetization (Szabó et al., 2007):

- MNP content and phase
- Average particle size of MNPs, size distribution, and aggregation state
- Specific surface area and the porous structure of clay
- Homogeneity dispersion of iron oxide crystals in the clay matrix.

Surface characteristics consist of hydrophobicity, specific surface area, pore distribution, and nanoparticle distribution are critical parameters of the nanocomposites. For adsorption and catalytic purposes for example, higher specific surface areas provide more space for adsorption. Synthesis method and route are important factors for designing the properties.

2. Synthesis of magnetic nanocomposites

2.1. Co-precipitation method

The synthesis of iron-based nanocomposites by co-precipitation method is the most efficient and straightforward

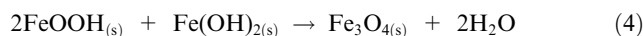
Table 1 Comparison properties of nature magnetic materials.

Iron oxide	Chemical formula	Color	Magnetic saturation $\text{A m}^2 \text{kg}^{-1}$	Grain size (nm)	Curie transition
Maghemite	$\gamma\text{-Fe}_2\text{O}_3$	Grey, grown, red	60–80	± 10	~820–980
Magnetite	Fe_3O_4	Black	92–100	± 6	~850
Hematite	$\alpha\text{-Fe}_2\text{O}_3$	Grey, grown, red	0.3	–	~1000

Table 2 The list of some commonly used magnetic source for producing iron-based nanocomposites by co-precipitation method.

Magnetic source	Modifier	Type of iron oxide	Reaction temperature (°C)	Reaction period	Solvent	Particle size (nm)	Magnetic saturation value (emu. g ⁻¹)	Application	Ref.
FeCl ₃ , FeSO ₄ ·7H ₂ O	Zn-Mn	Magnetite	80	20 min	Water	13	74	Hyperthermia	(de Mello et al., 2019)
FeCl ₃ , FeSO ₄ ·7H ₂ O	Egg shell	Magnetite	40	2 h	Water	24	14.46	Cr removal	(Sundararaman, 2020)
Fe(NO ₃) ₃ ·9H ₂ O	Ho(NO ₃) ₃ ·5H ₂ O	Hematite	78.3	60 min	Ethanol	25–30	0.71	Catalyst	(Nguyen et al., 2020)
FeCl ₃	SnCl ₂ ·2H ₂ O	Magnetite	100	30 min	Ethylene glycol	4.85	49.7	NA	(Radoń et al., 2020)
FeCl ₃ ·6H ₂ O	NiCl ₂ ·6H ₂ O/ZnCl ₂	Ferrite	NA	15 min	Water	NA	NA	NA	(Yi et al., 2019)
FeCl ₃ ·6H ₂ O	ZnCl ₂	Ferrite	80	40–60 min	Water	19	12	Hyperthermia	(Ait Kerroum et al., 478 (2019))
Fe ₂ (SO ₄) ₃ ·5H ₂ O/ FeSO ₄ ·7H ₂ O	Ce ⁴⁺ , Co ²⁺ , Mn ²⁺ , Ni ²⁺	Magnetite	70	30 min	Water	78.42	10.39	Photocatalyst	(Andrade Neto et al., 242 (2020))
FeCl ₃ , FeCl ₂	Sucrose	Magnetite	NA	NA	Water	4	17	NA	(Jesus et al., 2020)
FeSO ₄ ·7H ₂ O, FeCl ₃ ·6H ₂ O	Malic acid	Magnetite	RT	15 min	Water	10–50	NA	NA	(Klencsár et al., 2019)
FeCl ₂ ·4H ₂ O, FeCl ₃ ·6H ₂ O	Cellulose	Hematite	30	2.5 h	Water	5–100	13.2	As removal	(Yu et al., 2013)
FeCl ₃ ·6H ₂ O	NiCl ₂ ·6H ₂ O/ZnCl ₂	Ferrite	NA	15 min	Water	NA	148.1	NA	(Peng et al., 2017)
FeSO ₄ , FeCl ₃ ·6H ₂ O	Biopolymer	Magnetite	70	25 min	Water	498	~30	Adsorbent	(Lassalle et al., 2011)
FeCl ₃	CoCl ₂ , porous carbon	Ferrite	RT	6 h	Water	NA	9.875	Phosphate removal	(Karthikeyan et al., 2020)
Fe(NO ₃) ₃ ·9H ₂ O	Zn(NO ₃) ₂ ·6H ₂ O, TiO ₂	Ferrite	90	2 h	Water	11	NA	Photocatalyst	(Chandrika et al., 2019)
FeCl ₃ ·6H ₂ O, FeCl ₂ ·4H ₂ O	Polydextrose sorbitol carboxyl methyl ether	Magnetite	70	40 min	Water	12.5	69.2	NA	(Li et al., 2017)

wet chemical route which is generally synthesized from its salt species like Fe^{2+} and/or Fe^{3+} in alkali solution as shown in Table 2. the precipitation process of $\text{Fe}^{3+}/\text{Fe}^{2+}$ salt depends on the pH of the solution which generally occurs at a pH range between 8 and 14 with the $\text{Fe}^{3+}/\text{Fe}^{2+}$ ratio at 2:1 under non-oxidizing conditions. The reaction of the synthesis of wet chemical route of magnetite nanoparticles is shown in Eq. (1)–(4).



Mello et al. (2019) synthesized the Zn-Mn-doped magnetite nanoparticles by co-precipitation method with the FeCl_3 and $\text{FeSO}_4 \cdot 7\text{H}_2\text{O}$ as the precursors with the average of particle size of 10–15 nm (de Mello et al., 2019). The authors reported that the type of precursors is a mainly factor in the synthesis of magnetite nanoparticles by co-precipitation method. In addition, the several factors that have affected the particle size of the prepared nanoparticles by this method are operating temperature, the absence or presence of the stabilizing agent, reaction time, and the pH (Mascolo et al., 2013). The doping with other metals like Zn^{2+} and Mn^{2+} can improve the magnetization properties compared to pure magnetite. In their research, the addition of Zn^{2+} and Mn^{2+} can change the crystal structure which affects the electron migration in the structure. The doping system has been widely reported that it can improve intrinsic properties, especially its permanent magnetic properties. For example, Li et al. (2019) reported that intrinsic properties of the microstructure of nanocomposites $(\text{La, Pr})_3\text{Fe}_{14}\text{B}$ is dependent on La content. The doping system with rare earth metal could improve the permanent magnetic properties (Li et al., 2019). Rare earth metal has an electron in orbital 4f that close with atomic core and show spin-orbit solid interaction. Therefore, the metal has been widely exploited as doping for producing permanent magnetic materials (Skomski et al., 2006).

Yu et al. (2013) prepared the magnetic composites of cellulose/iron oxide nanoparticles in the NaOH -thiourea-urea- H_2O at operating temperature of 30 °C (Yu et al., 2013). The solution is used to increase the dissolution of cellulose chains in the preparing nanocomposites. The presence of magnetite nanoparticles can increase the specific of surface area until 100-fold with

the average particle size of 61 nm in the cellulose matrix. Although, the cellulose is non-conductive polymer, however the nanocomposite shows the sensitive-magnetic induced with the magnetization value of 13.2 emu g^{-1} . In their research, the synthesized nanocomposite has been applied for removing the heavy metal ions. With the presence of cellulose in the composite structure, the material exhibited a high adsorption capacity for As^{3+} due to the presence of functional group like hydroxyl (OH^-). In other words, beside the addition of organic material for arranging the size, several studies also have reported that the shape and particle size of iron-based nanoparticles in the matrix composites can be controlled by adjusting ionic strength, pH, temperature, and type of salts (nitrates, acetates, chlorides, and sulfates) (Gnanaprakash et al., 2007; Yang et al., 2012). However, the ratio of precursors salts is a major factor to produce the high percentage of yields and desirable size of nanoparticles (Ramimoghadam et al., 2014). In fact, the previous studies have revealed that the increasing ratio of $\text{Fe}^{3+}/\text{Fe}^{2+}$ can produce the larger particle size of nanoparticles. In other words, based on the previous research, the smaller particle size will be obtained under high pH conditions and ionic strength (Tartaj et al., 2004). Besides that, another study also reported and revealed that the temperature significantly increased the particle size of iron oxide nanoparticle due to the formation of goethite phase (Gnanaprakash et al., 2007). The co-precipitation method offers a high quantity of products; however, the produced material has not uniform size particle distribution (Liu et al., 2019).

2.2. Chemical vapor deposition (CVD)

Chemical vapor deposition (CVD) has proved that the method can produce the iron oxide nanocomposites with high performance as a solid material, produced one-dimensional nanomaterials, and high purity. This method is commonly used in a chamber with a reactive gas which can deposit on a substrate to produce a coating material. Moreover, this method offers high flexibility in producing material because of many databases reported (Majidi et al., 2016). Atchudan et al. (2019) reported a simple method for synthesis of iron oxide nanoparticles filled multi wall carbon nanotubes (IONP/MWCNTs) by CVD method (Atchudan et al., 2019). The results confirmed that the IONPs inside in the MWCNTs which have the narrow distribution of diameter at 9 nm. The authors reported that the purified materials could be done by washing the produced material with a simple acid etching method, while the other methods that have been reported the purified materials com-

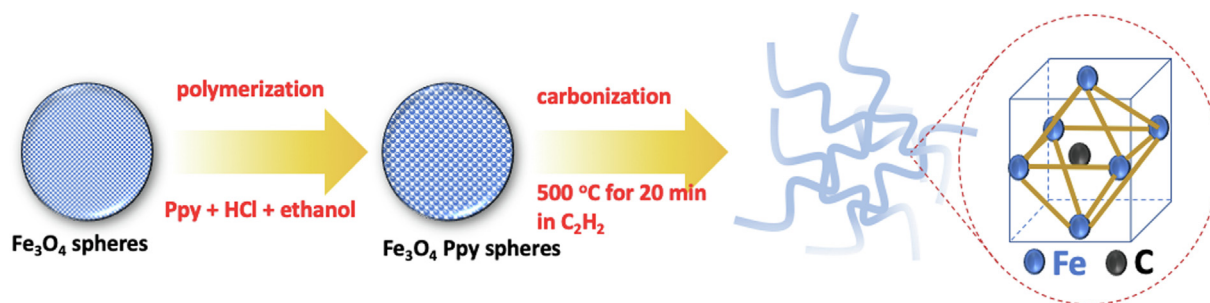


Fig. 1 The representative of the synthesis of iron-based nanocomposite materials using the organic molecules as modifier (Chen et al., 2020).

Table 3 The list of some commonly used magnetic source for producing iron-based nanocomposites by CVD methods.

Magnetic source	Modifier	Type of iron oxide	Reaction temperature (°C)	Reaction period	General Remarks	Particle size (nm)	Magnetic saturation value (emu. g ⁻¹)	Application	Ref.
Fe(CO) ₅	Alloy (Na, Ga, B)	NA	120	30 min	Ar atmosphere	50–100	NA	NA	(Jun et al., 2013)
Fe(NO ₃) ₃ ·9H ₂ O	CNTs	Goethite	700	30 min	Ar and CH ₄ atmosphere	40–60	13.79	Pb removal	(Alijani et al., 2014)
Fe(acac) ₃	MWCNTs	Magnetite	800	30 min	Ar and C ₂ H ₂ atmosphere	NA	NA	Capacitors	(Atchudan et al., 2019)
Fe pure	3-triethoxysilypropylamine, paracyclophane dimer	NA	650	NA	Vacuum atmosphere	65	125.8	Coating layer	(Zhang et al., 2020)
Fe ₃ (CO) ₁₂	Fe/Fe oxides/metal oxide	Magnetite	450	40 min	Prepressure at 10 ^{-3/-4} Pa without using any carrier gas	3	NA	NA	(Vangelista et al., 2012)
Ni _{0.5} Zn _{0.5} Fe ₂ O ₄	MWCNTs	Hematite	750	30 min	Ar atmosphere	~50	NA	MW absorber	(Mustaffa et al., 2019)
Fe(hfa) ₂ TMEDA (hfa = 1,1,1,5,5,5-hexafluoro-2,4-pentanedionate; TMEDA = N,N,N',N'-tetramethylethylenediamine)	Au metal	Ferrite	400	60 min	Dry O ₂ (P = 3.0 mbar)	end	NA	NA	(Maccato et al., 2018)
FeCl ₃ ·6H ₂ O	CNFs/Polypyrrole	Magnetite	500	20 min	C ₂ H ₂ atmosphere	50–60	NA	Energy storage	(Chen et al., 2020)
FeCl ₃	Carbon	Magnetite	450	10–30 min	C ₂ H ₂ atmosphere and Ar carry gas	< 100 nm	NA	Energy storage	(Wang et al., 2015)
Fe(NO ₃) ₃ ·9H ₂ O	Co ²⁺	Ferrite	700	30 min	C ₂ H ₂ atmosphere and N ₂ carry gas	500	2.61	Catalyst	(Dhand et al., 2017)

Table 4 The list of some commonly used magnetic source for producing iron-based nanocomposites by electrochemical methods.

Magnetic source	Modifier	Type of iron oxide	Reaction temperature (°C)	Reaction period	General Remarks	Particle size (nm)	Magnetic saturation value (emu. g ⁻¹)	Application	Ref.
Fe pure	NA	Magnetite	RT	4 h	LiCl-C ₂ H ₅ OH solution, Potential at 0,4 V	40	35.5	NA	(Starowicz et al., 2011)
Fe metals	NA	Magnetite	RT	10 min	((CH ₃) ₄ NCl) and NaCl in ethanol:water (1:1)	8–13	86.85	NA	(Marín et al., 2016)
(NH ₄) ₂ Fe(SO ₄) ₂ (H ₂ O) ₆	Graphene	Magnetite, maghemite	RT	3 h	HCl-H ₂ O solvent, Potential at 10 V, SDSs as surfactant	20–30	57.3	NA	(Ansari et al., 2020)
FeCl ₃ ·6H ₂ O	Triethanolamine	Maghemite	RT	2 h	NaOH solution	450	84.40	Supercapacitor	(Elrouby et al., 2017)
Sponge Iron	NA	NA	30–50	> 10 h	Working electrode at 1 cm ² OH ⁻ solution	NA	NA	NA	(Sun et al., 2018)
Iron rods	Ethylene glycol	Magnetite, hematite	RT	15 min	Ammonium fluoride solution, Potential at 50 V	NA	NA	Water splitting	(Lucas-Granados et al., 2018)
Iron metals	1, 3, 5- benzenetricarboxylic acid (BTC)	NA	NA	NA	Potential at 12 V	100–200	NA	As removal	(Zhang et al., 2018)
FeSO ₄	Polyvinyl alcohol, CNTs	Magnetite	RT	3 h	The current density at 348 mA cm ⁻²	33	NA	Antibacterial	(Sadeghfar et al., 2018)
FeSO ₄ ·7H ₂ O	MWCNTs	NA	NA	NA	Na ₂ SO ₄ solution	50	NA	Catalyst	(Torabi and Sadrnezhad, 2010)
Iron plate	Hexagonal mesoporous spheres (HMS)	NA	RT	3 h	Na ₂ S ₂ O ₃ solution	> 200	2.9	NA	(Wang et al., 2007)

monly used the mixture of nitric acid and hydrochloric acid. Chen et al. (2020) studied the Fe₃C/N-doped carbon nanofibers nanocomposites by CVD as lithium storage anode. In this method, the nanocomposites was prepared at low annealing temperature with Fe₃O₄ as iron source and acetylene as carbon source (Chen et al., 2020). The microstructure and morphology of the prepared material showed that the material has ununiform diameter at 50–60 nm. Their studies proved that the diameter of nanomaterials can be controlled by the addition of some organic compounds like surfactant or hydrophilic/hydrophobic molecules when the synthesis process. The presence of organic molecules like surfactants plays an important role in the controlling of particle size on the dispersion and stability of solution (Ordóñez et al., 2020). However, the high modifier on the composites also can decrease the pore volume of the prepared materials due to the agglomeration process. Fig. 1 shows the illustration of the synthesis of iron-based nanocomposite materials.

Ren et al. (2018) reported the synthesis of amorphous iron (III) phosphate/carbon nanotubes (FePO₄/CNTs) at low processing temperature (~300 °C) and low vacuum conditions (4–8 Torr) (Ren et al., 2018). The authors proved that the temperature is an essential factor for the decomposition of precursors on the substrate. At temperature less than 250 °C, the precursors did not decompose and slowly deposition on the substrate. Besides the temperatures, the other factors that have affected the synthesis process by CVD such as the processing time, the gas flow rate, the catalyst, and also the precursors (Lopez et al., 2015). However, recently, the CVD is probably the most versatile synthesis method for producing iron-based nanocomposites because this method offers several advantages such as cheap and simple method for mass production of nanomaterials, and it can be used to grow the different forms of nanostructure. Table 3 shows the list of some commonly used magnetic source for producing iron-based nanocomposites by CVD methods (Shah and Tali, 2016).

2.3. Electrochemical synthesis

Electrochemical method has been widely used for generating synthesis of iron-based nanocomposites with different phases of iron oxide like magnetite and maghemite as shown in

Table 4. In general, electrochemical synthesis can be done by passing an electric current between two or more electrodes called anodes and cathodes on the electrolyte solution medium. In this technique, the anode metal will be oxidized into its ion species and then the ion will be reduced by the cathode to metal with the presence of stabilizers. In fact, electrochemical synthesis occurs at the interface of electrolyte and electrode and form electric double layers. This method can highly produce a large percent yield of products compared to the chemical synthesis routes. Ansari et al. (2020) studied the synthesis of iron/graphene composites with electrochemical exfoliation using a surfactant as stabilizers to produce nanoparticles (Ansari et al., 2020). The authors presented that the surfactant is a major component in the synthesis of iron oxide nanocomposites because it can control the stabilization of the iron species in the electrolyte solution and can reduce their oxidization by the dissolved oxygen. However, the increasing concentration of surfactants can reduce the magnetization properties of the composites by forming a layer on the surface of the nanoparticles which causes the agglomeration process (Haramagatti et al., 2018). Besides, the presence of surfactants as stabilizer, several factors affect the process of electrosynthesis of iron-based nanocomposites such as type of both electrodes (anode and cathode), the type and concentration of electrolyte solution, temperature, pH, and also electrolysis type (galvanostatic or potentiostatic) (Ramimoghdam et al., 2014). However, two key factors that influence the reaction process that occurs are the cell potential and the current applied which can be changed during the reaction as a function of time.

Starowicz et al. (2011) revealed that the particle size of iron-based nanoparticles can be controlled by the type of electrolyte solution (Starowicz et al., 2011). In the water medium, the particle size of iron nanoparticles has an average size of nanoparticles between 20 and 40 nm, while at the presence of another solvent like ethanol, the particle size can be obtained less than 20 nm. The electrosynthesis of iron-based nanoparticles can be conducted in constant current (galvanostatic), at this condition the iron will be oxidized in anode electrode while in the cathode electrode will be produced the hydroxyl ion (OH⁻). Then, the iron ion produced will lead to form Fe(OH)₂ which will be converted to iron oxide through the Schikorr reaction $3\text{Fe}(\text{OH})_2 \rightarrow \text{Fe}_3\text{O}_4 + 2\text{H}_2\text{O} + \text{H}_2$. Based on the principle, the

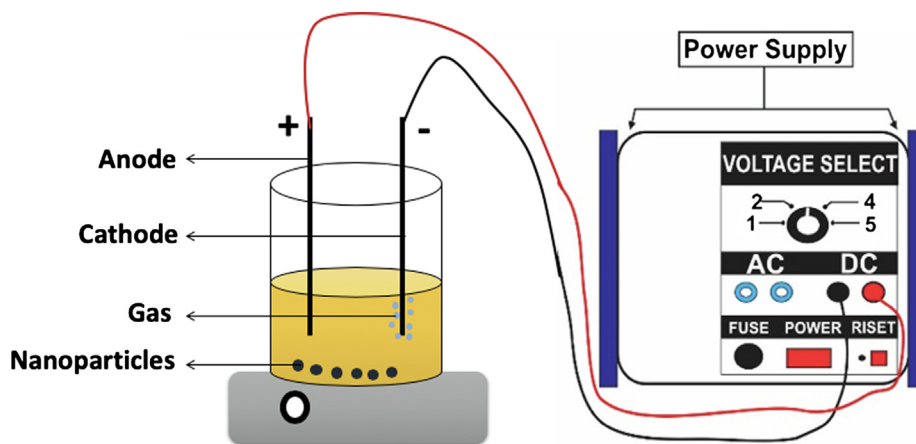


Fig. 2 The illustration of electrochemical synthesis of iron-based nanoparticles.

Table 5 The list of some commonly used magnetic source for producing iron-based nanocomposites by solvothermal methods.

Magnetic Source	Modifier	Solvent	Reaction Temperature (°C)	Reaction Period	Particle Size (nm)	Magnetic Saturation Value (emu.g ⁻¹)	Iron Form	Application	Classification	Ref.
Fe(acac) ₃	Cu ²⁺	Triethylene glycol	260	24 h	19.9	53.1	Magnetite	Magnetic fluid hyperthermia	Metal Oxide-based Material	(Fotukian et al., 2020)
FeCl ₃ ·6H ₂ O	Mn ²⁺ , Carbonyl Iron (CI)	Ethylene glycol, Silicone Oil	200	12 h	21.4	58.8	Magnetite	MR Fluids (Smart Material)	Metal Oxide-based Material	(Wang et al., 2020)
FeCl ₃ ·6H ₂ O	Trisodium Citrate (TSC) Dihydrate	Ethylene glycol	200	10 h	280	70.2	Magnetite	Identification of glycopeptides in human saliva	Metal Oxide-based Material	(Chu et al., 2020)
FeSO ₄ ·7H ₂ O	Zn ²⁺ , Mn ²⁺ , Bi ³⁺ , TEOS	Ethylene glycol	180	5 h	60	17.72	Magnetite	Adsorption and photocatalytic degradation of dyes	Metal Oxide-based Material	(Kaewmanee et al., 2020)
FeCl ₃ , and FeCl ₂	Biomass-based Carbon, and Graphene	Water, Ethanol	260	2 h	5–20	14.28	Magnetite and Maghemite	NA	Graphene-Mixed Carbon Material	(Siddiqui et al., 2020)
FeCl ₃ ·6H ₂ O	Mn ²⁺ , Graphene Oxide (GO)	Ethylene glycol, PEG-2000	200	10 h	30–100	25.5	Magnetite	Photocatalytic degradation of dye	Reduced Graphene Oxide-Based Material	(Huang et al., 2019)
FeCl ₃ ·6H ₂ O, FeCl ₃ ·4H ₂ O	Graphene oxide (GO), chitosan	Ethylene glycol	180	12 h	~ 250	46.5	Magnetite and Hematite	Adsorption of aromatic compounds	Graphene-Mixed Carbon Material	(Rebekah et al., 2020)
FeCl ₃ ·6H ₂ O	Mg ²⁺ , Al ³⁺ , Graphene oxide and C ₂ H ₈ N ₂	Ethylene glycol	200	8 h	5–10	~ 18	Magnetite	Adsorption of metal ions	Graphene Oxide-Based Material	(Huang et al., 2018)
FeCl ₃ ·6H ₂ O, FeSO ₄ ·7H ₂ O	Ti ⁴⁺ , Graphene oxide	Isopropanol	180	16 h	100–500	2.74–8.89	Magnetite	Photocatalytic ozonation	Graphene Oxide-Based Material	(Chávez et al., 2020)
Fe(C ₅ H ₅) ₂	N/A	Hydrogen Peroxide, Acetone	200	48 h	5.6–18.6	26.8	Magnetite	Photocatalytic degradation	Carbon-Based Material	(Zhang et al., 2020)
C ₁₅ H ₂₁ FeO ₆ , Co	Spherical activated carbon (SAC)	Benzyl Alcohol, Methanol, C ₄ H ₆ N ₂ (Hmim)	175	48 h	200–400	8.2	Magnetite	Catalyst for Knoevenagel condensation	Activated Carbon-Based Material	(Xiang et al., 2020)
(NO ₃) ₂ ·6H ₂ O	Mn ²⁺ , Glucose, Amine – NH ₂	Ethylene glycol, polyethylene glycol	200	12 h	40	26.5	Magnetite	Heterogeneous Fenton catalyst	Carbon-Based Material	(Qin et al., 2020)

Table 5 (continued)

Magnetic Source	Modifier	Solvent	Reaction Temperature (°C)	Reaction Period	Particle Size (nm)	Magnetic Saturation Value (emu.g ⁻¹)	Iron Form	Application	Classification	Ref.
Fe(C ₅ H ₅) ₂	PF-127, C ₁₀ H ₆ (OH) ₂	Ethanol, Hydrogen Peroxide	220	24 h	~306	5.7–26.38	Magnetite	Adsorbent of organic pollutant	Carbon-Based Material	(Cui et al., 2020)
FeCl ₃ ·6H ₂ O, FeSO ₄ ·7H ₂ O	Biomass-based Carbon	Water	230	24 h	~ 10–20	9.73	Magnetite	Adsorption of Tetracycline	Activated Carbon-Based Material	(Rattanachueskul et al., 2017)
FeCl ₃ ·6H ₂ O, FeSO ₄ ·7H ₂ O	Biomass-based carbon	Water	200	24 h	~ 300	15.58	Hematite	Adsorption of Mercury	Activated Carbon-Based Material	(Wang et al., 2018)
FeCl ₃ ·6H ₂ O, FeSO ₄ ·7H ₂ O	Starch-based carbon	Water, NH ₄ OH	200	12 h	~ 2–10	~ 130	Magnetite	Biomedical application	Carbon-Based Material	(Lee et al., 2019)
FeCl ₃ ·6H ₂ O	3D carbon nanofiber, Dopamine hydrochloride	Ethylene Glycol, PEG-2000	200	8 h	~ 200–250	13.4–39.7	Magnetite	Electromagnetic shielding	Carbon-Based Material	(Zhan et al., 2018)
FeCl ₃	Biomass-based carbon	Diethylene Glycol (DEG)	200	24 h	~ 10–11	11.9–22.7	Magnetite	Adsorption and Fenton degradation of dye	Activated Carbon-Based Material	(Liu et al., 2017)
FeCl ₃ ·6H ₂ O	MCNTs, SDBS	Ethylene Glycol	180	8 h	400	~ 50–60	Magnetite	Microwave adsorption and Supercapacitor	Carbon-Based Material	(Zeng et al., 2020)
FeCl ₃ ·6H ₂ O	Ni ²⁺ , Carbon Paste, Graphite Powder, Paraffin oil	Ethanol, Ethylene Glycol, PEG	160	7 h	31	70–80	Magnetite	Electrochemical sensor	Carbon-Based Material	(Tajyani and Babaei, 2018)
FeCl ₃ ·6H ₂ O	Glucose, Ammonia	Ethylene Glycol, PEG	200	6 h	138–416	40	Magnetite	Laccase immobilization	Carbon-Based Material	(Lin et al., 2017)
FeSO ₄ ·4H ₂ O	C ₃₁ H ₂₈ O ₁₂	Water	160	8 h	~ 40–80	~ 25	Magnetite	Adsorption of heavy metal ions	Natural Polymer-Based Material	(Shi et al., 2020)
FeCl ₃ ·6H ₂ O	Montmorillonite, Hexandiamine	Ethylene Glycol	198	6 h	30–50	15	Magnetite	Adsorption of heavy metal ions	Clay-Based Material	(Irawan et al., 2019)
FeCl ₃ ·6H ₂ O	Bentonite, C ₂ H ₄ (NH ₂) ₂	Ethylene Glycol	200	8 h	10–50	15.1–37.4	Magnetite	Adsorption of heavy metal ions	Clay-Based Material	(Yan et al., 2016)
FeCl ₃ ·6H ₂ O, CoCl ₂ ·6H ₂ O	Mn ²⁺ , Bentonite, APTES	Ethylene Glycol	200	12 h	~ 110	7	Magnetite	Adsorption of heavy metal ions	Clay-Based Material	(Zhou et al., 2019)
FeCl ₃ ·6H ₂ O, FeSO ₄ ·7H ₂ O	Halloysite, Carbon paste, Graphite powder, Paraffin oil	Water	105	12 h	~ 30–50	25.1	Magnetite	Electrochemical detection of Hg (II)	Clay-Based Material	(Fayazi et al., 2016)

water medium plays an important role to generate the production of iron hydroxyl species. However, in the pure water medium, the process will occur at a high rate so that the presence of ethanol in the water can regulate the water concentration and reduce the formation rates which can produce smaller particle sizes (Karimzadeh et al., 2016). The electrochemical method offers some advantages in iron oxide synthesis such as easily controlling size distribution and high production rate; however, this method is difficult to control the high crystallinity of the produced material (Setyawan and Widiyastuti, 2019). Fig. 2 shows the illustration of electrochemical cell for synthesis of iron-based nanoparticles.

2.4. Solvothermal method

Synthesis of magnetic nanomaterials, classifications, and its applications by solvothermal method have been presented in the literature Table 5. The solvothermal method is one of the well-known techniques in the fabrication of magnetite materials. This method is almost similar to the hydrothermal method in the synthesis procedure, except the use of water as a solvent is replaced by an organic solvent (Feng et al., 2017). The solvothermal method is sometimes referred to the alcoholothermal and glycolthermal method when the class of alcohol and glycerol are used as a solvent in the reaction (Erdemi and Baykal, 2015). In fact, there have been many experiments using both classes of solvents, where this is an important strategy to control the shape, phase, and size distribution of crystal in magnetite materials. The physical properties of magnetite materials can be adjusted using several parameters such as the type of precursor, solvent, temperature and reaction time (Kefeni et al., 2017). In the one-step supercritical synthesis of magnetic iron nanoparticles, pressure and temperature conditions facilitate the product crystallization process through the dissolution and diffusion of iron salts. The reaction mechanisms are naturally highly system dependent. The aqueous solution of the iron salt is brought to its subcritical temperature, and the low dielectric constant will instantly force the nanoparticles to precipitate so that nucleation occurs instantaneously. Then tiny and homogeneous iron particles with a very

narrow size distribution obtained from the simultaneous deposition of numerous iron nuclei (Nunes et al., 2019).

The solvothermal process of most common magnetic material is carried out through the process of hydrolysis and oxidation of iron salt solutions as a precursor or neutralization process of mixed metal hydroxides in aqueous media which can cause the formation of ferrite. During the solvothermal process, the chemical reaction between the precursor and the solvent takes place in a sealed autoclave reactor at very high temperature (ca. 130–250 °C) and autogenous pressure (ca. 0.3–4 MPa) (Sharifianjazi et al., 2020; Qiao et al., 2019). This condition can increase the solvent ability to dissolve the precursors and accelerate the formation of products.

For example, Fotukian et al. (2020) successfully synthesized of Fe_3O_4 and monodisperse CuFe_2O_4 with triethylene glycol as the solvent and stabilizer for the application of magnetic fluid hyperthermia through solvothermal process at 260 °C for 24 h. The obtained Fe_3O_4 and CuFe_2O_4 exhibited very small particles size with great superparamagnetic properties. Another experiment was conducted by Huang et al. (2019) to fabricate magnetically separable reduced graphene oxide supported MnFe_2O_4 hybrids (rGO/ MnFe_2O_4) by one-pot solvothermal synthesis for photocatalytic degradation of dye. The results show that the rGO nanosheets was embedded by monodisperse MnFe_2O_4 with uniform particles size. In the general procedure, the appropriate proportions of precursors and solvents are inserted into the sealed autoclave reactor and then placed in the oven at a predetermined temperature and time as shown in Figs. 3 and 4. Therefore, the solvothermal method can be used to control the shape and size of nanoparticles, also to improve physical and chemical properties of magnetic materials which can be utilized for industrial and biomedical applications. Some of the significant advantages of hydro/solvothermal synthesis are the use of appropriate eco-friendly solvents for the nucleation of homogeneous particles, the chemical activity of the reactant improve, intermediate and metastable products may be quickly produced, easy and precise control of the size, shape distribution, and crystallinity of the final product. While some of the disadvantages of this method are the need for quite an expensive autoclave, safety



Fig. 3 The synthesis of Fe_3O_4 and monodisperse CuFe_2O_4 through solvothermal method by Fotukian et al. (2020).

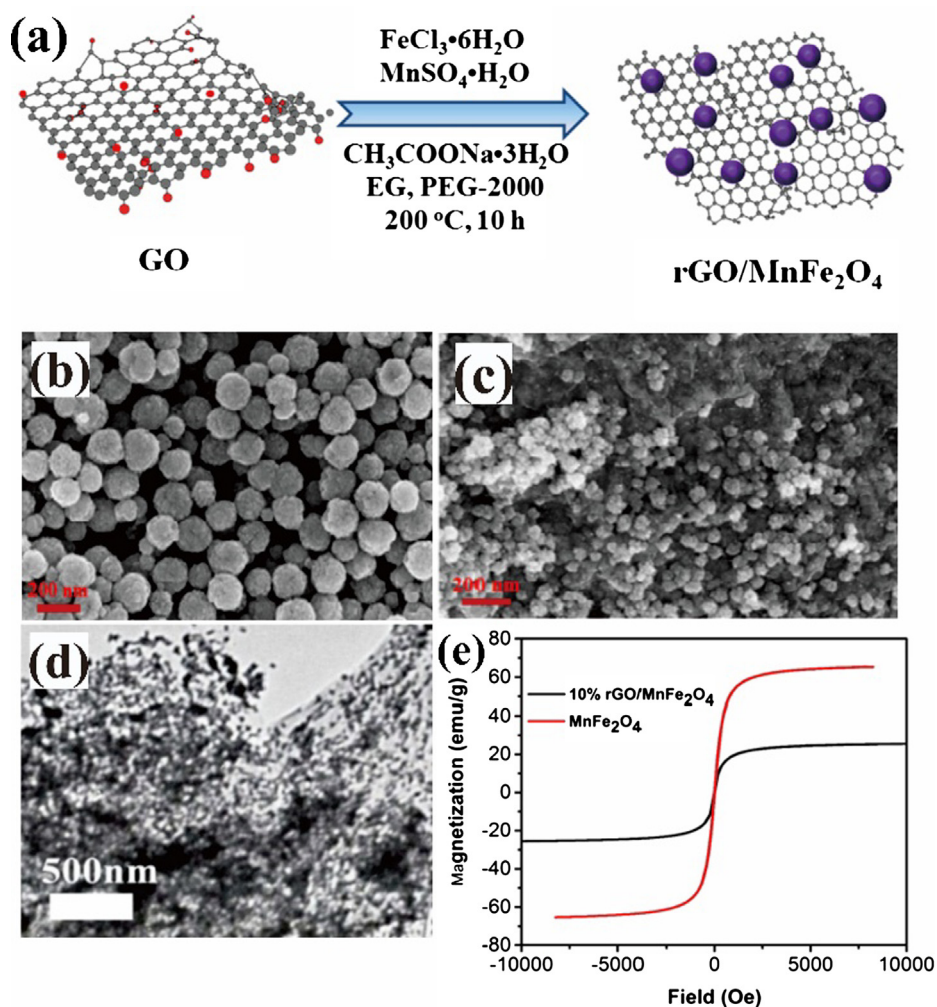


Fig. 4 (a) A synthesis model of magnetically separable reduced graphene oxide supported MnFe_2O_4 hybrids ($\text{rGO}/\text{MnFe}_2\text{O}_4$) by one-pot solvothermal synthesis by Huang et al. (2019); SEM images: (b) pure MnFe_2O_4 and (c) 10% $\text{rGO}/\text{MnFe}_2\text{O}_4$; TEM image of (d) 10% $\text{rGO}/\text{MnFe}_2\text{O}_4$ and (e) Hysteresis loops comparison of pure MnFe_2O_4 and 10% $\text{rGO}/\text{MnFe}_2\text{O}_4$.

issues during the reaction process, and the impossibility of observing the reaction process (Rane et al., 2019).

2.5. Microemulsion

Synthesis of magnetic nanomaterials, classifications and its applications by microemulsion method have been presented in the literature Table 6. Microemulsion is a stable colloidal suspension in two phases which do not dissolve each other and combine into one phase with the help of surfactants (such as Tween 80, sodium dodecyl sulphate, brij, etc.). The microemulsion solvent can be either the water/oil (w/o) or oil/water (o/w) system (Qiao et al., 2019). While magnetic nanoparticle precursors are dispersed into aqueous phase with the size of 1–100 nm. The microemulsion mechanism begins with the formation of a micelle system as a nanoreactor caused by water droplets containing magnetic nanoparticles encircled by surfactant molecules. Nucleation, growth and agglomeration of magnetic nanoparticles are restricted by micelle layers.

After that, the second emulsion is added to the solution to precipitate magnetic nanoparticles (Sharifianjazi et al., 2020).

For example, the synthesis process of core-shell $\text{Fe}_3\text{O}_4@-\text{SiO}_2$ nanoparticles using the reverse microemulsion method. In this method, one or two surfactants become stabilizers of the hydrolysis reaction and condensation in water droplets that contain magnetic material precursors that are well dispersed in the organic phase. Therefore, the aggregation process can be prevented when the formation of silica layers on the magnetic surface of nanoparticles happens (Asgari et al., 2019). Lv et al. (2015) revealed the novel synthesis of Fe_3O_4 particles pagoda-like microstructures using the microemulsion-assisted hydrothermal method for the application of Lithium-air batteries. The experimental results show that the increase in reaction time is very influential on the morphological evolution of samples from pagoda-like to flower-like shapes. In addition, the concentration of NaOH and polyethylene glycol (PEG)-2000 has a major role in the morphology of the final product.

Table 6 The list of some commonly used magnetic source for producing iron-based nanocomposites by microemulsion methods.

Magnetic Source	Modifier	Solvent	Reaction Temperature (°C)	Reaction Period	Particle Size (nm)	Magnetic Saturation Value (emu.g ⁻¹)	Iron Form	Application	Classification	Ref.
FeCl ₃ , FeCl ₂	Mn ²⁺ , Zn ²⁺ , S ²⁻ , SDS and TEOS	Water, Toluene, Isopropanol	60	NA	45	31.7	Magnetite	Drug delivery system	Metal Oxide-based Material	(Dung et al., 2016)
K ₄ [Fe(CN) ₆]	NaOH, Hydrazine	Water, PEG-2000, Triton X-100, Amyl alcohol, Cyclohexane	180	20 h	200–600	NA	Magnetite	Lithium-Air battery	Metal Oxide-based Material	(Lv et al., 2015)
FeCl ₃	TEOS, SDBS, Pyrrole (Py), Trisodium citrate (TSC) Dihydrate	Water, Ethanol, Ethylene Glycol	4	12 h	110–240	0.02–0.48	Magnetite	Microwave absorber	Polymer-based Material	(Liu et al., 2019)
Fe(acac) ₃	Oleic acid, Oleylamine, CTAB, Urea	Water, Chloroform, Cyclohexane, Dibenzylether, Butanol	120	12 h	16.4	4.8	Magnetite	Drug delivery system	Silica-based Material	(Asgari et al., 2019)
FeCl ₃ ·6H ₂ O	Sr ²⁺ , CTAB, TEOS	Water, Butanol, Isooctane	RT and 1050	24 h and 4 h	6.6	18.4	ε-Fe ₂ O ₃ , Magnetite, Hematite	NA	Silica-based Material	(Nikolic et al., 2017)
FeCl ₃ , FeCl ₂ ·4H ₂ O	Ta ⁵⁺ , PVP, Dipicolinic acid	Water, Hexane	25	15 min	38	6.58	Magnetite	Lipase immobilization	MOF-based Material	(Sargazi et al., 2018)
FeCl ₃ ·6H ₂ O	Oleic acid and Sodium oleate	Water, Ethanol, Hexane, Octadecene	20 and 320	30 min and 24 h	~ 8–18	~ 6–21	Magnetite	Magnetic fluid fields	Metal Oxide-based Material	(Yu et al., 2018)
FeCl ₃ ·6H ₂ O, (NH ₄) ₂ Fe(SO ₄) ₂ ·6H ₂ O	Fatty Acids (C ₆ -C ₁₁)	Water, Acetone	80	30 min	8–12	NA	Magnetite	Adsorption of PAHs compound	Metal Oxide-based Material	(Liao et al., 2015)
FeCl ₃ ·6H ₂ O	Ca ²⁺ , Mg ²⁺ , Brij-35	Water, Hexane, Butanol	500–900	180 min	40–100	~ 6–9.5	Magnetite	Drug delivery system	Calcium-based Material	(Foroughi et al., 2016)
NiCl ₂ ·6H ₂ O, FeCl ₂ ·4H ₂ O	CTAB, Hydrazine	Water, Hexanol, Octane, Butanol	70	60 min	~ 7	11.4	Magnetite	NA	Metal Oxide-based Material	(Beygi and Babakhani, 2017)
NH ₄ Fe(SO ₄) ₂ ·12H ₂ O, (NH ₄) ₂ Fe(SO ₄) ₂ ·6H ₂ O	Ag ³⁺ , CTAB, Glucose	Water	50	24 h	~ 9–11	53	Magnetite	NA	Metal Oxide-based Material	(Singh and Upadhyay, 2018)
FeCl ₃ ·6H ₂ O, FeSO ₄ ·7H ₂ O	TMAAC, Sodium citrate, Chitosan	Water, Atolin, Span-80, Tween-80	60	60 min	< 10	21.57	Magnetite	Adsorption of dye	Polymer-based Material	(Yu et al., 2016)
Fe(acac) ₃	TEOS, CTAB, Oleic acid	Water, Benzyl ether, Chloroform, Ethanol	70	30 min	220–260	39.7	Magnetite	Adsorption of metal ion	Silica-based Material	(Meng et al., 2018)
FeCl ₃ ·6H ₂ O, FeCl ₂ ·4H ₂ O	ω-TA, Benzoyl peroxide, PVA, DTAC, Glutaraldehyde	Water, Butanol, Ethanol	70	7 h	30–40	47.84	Magnetite	Biocatalyst	Polymer-based Material	(Jia et al., 2016)

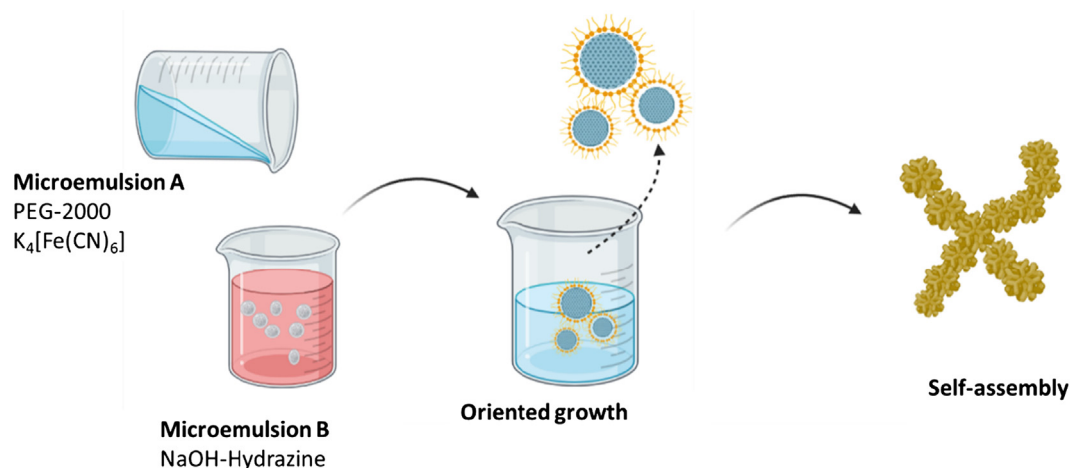


Fig. 5 Schematic representation of the self-assembly in Fe_3O_4 particles synthesis (adapted from Lv et al., 2015).

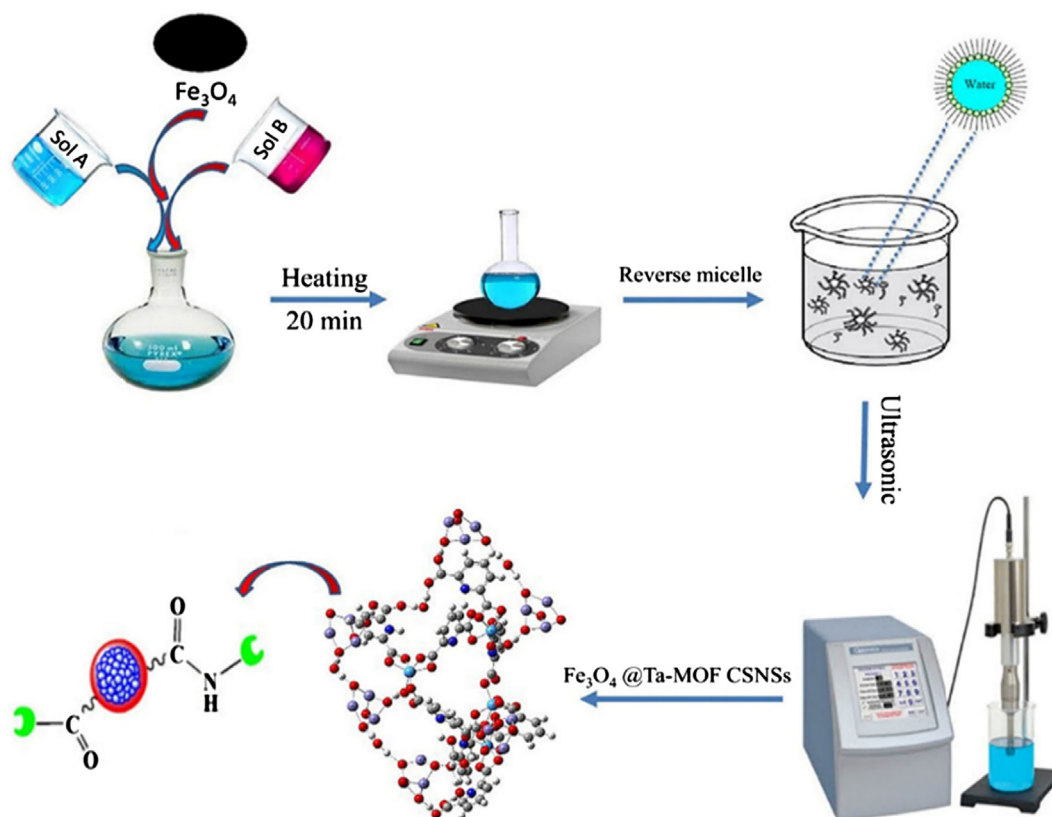


Fig. 6 The synthesis of Ta-MOF@ Fe_3O_4 nanostructures via ultrasound assisted reverse micelle (UARM) by Sargazi et al. (2018).

Asgari et al. (2019) synthesized the core-shell structure of monodisperse magnetic mesoporous silica nanoparticles (MMSN) via inverse microemulsion method for anticancer drug carriers. In that study, Fe_3O_4 in urea solution acts as a water phase, silica precursors in cyclohexane as an oil phase, as well as cetyltrimethylammonium bromide (CTAB) and 1-butanol as surfactants and co-surfactants, respectively. This method is different from the conventional inverse microemulsion method because the magnetic precursors used will be coated by CTAB and oleic acid as surfactants in the core-

phase, then silica formation in shell-phase. The experimental results reveal that the increase in reaction temperature from 70 to 120 °C affects the increase in the thickness of the silica layer as the shell-phase from 3 to 17 nm.

Another experiment by Sargazi et al. (2018) exhibited the synthesis of Ta-MOF@ Fe_3O_4 core/shell nanostructures through novel ultrasound-assisted reverse micelle (UARM) method in optimum conditions for a novel candidate for enzyme immobilization. The obtained product from this experiment has the particle size distribution of 38 nm, thermal sta-

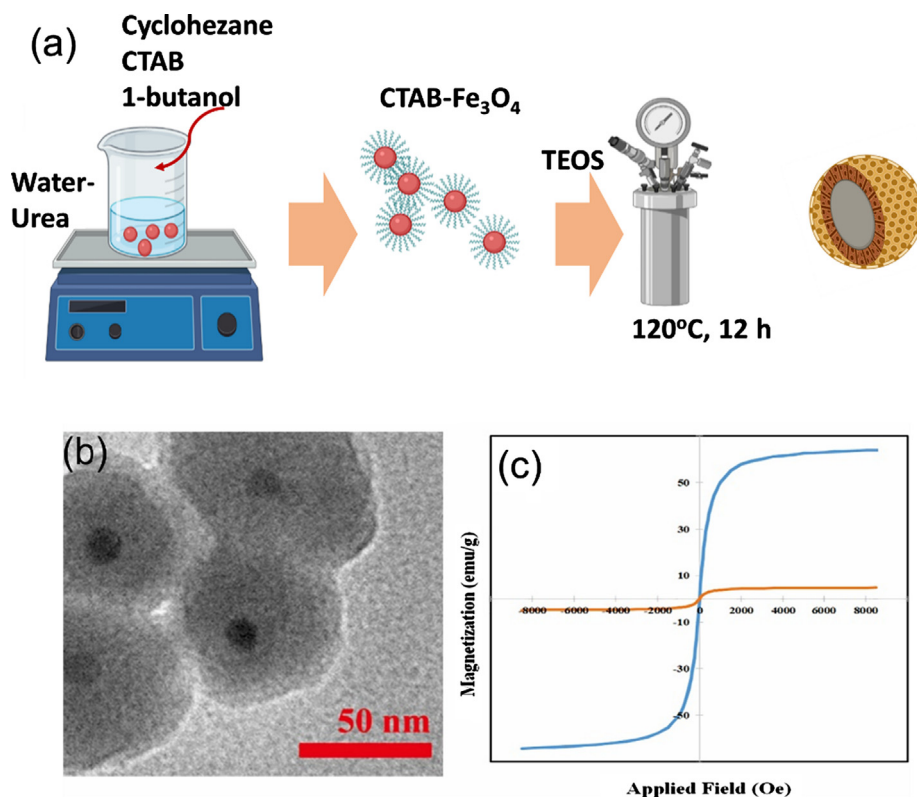


Fig. 7 (a) The synthesis route of $\text{Fe}_3\text{O}_4@m\text{SiO}_2$ nanoparticles via modified inverse microemulsion technique by [Asgari et al. \(2019\)](#); (b) TEM image of naked Fe_3O_4 nanoparticles; (c) Hysteresis loops of $\text{Fe}_3\text{O}_4@oleic\ acid$ (blue) and $\text{Fe}_3\text{O}_4@m\text{SiO}_2$ (orange).

bility at 200°C and a large surface area. The SEM image of Ta-MOF@ Fe_3O_4 core/shell reveals that the targeted enzyme is stably and efficiently loaded on the material substrate. Therefore, the method used and the obtained results can be developed for the application of other compounds in biology.

Some of the microemulsion synthesis methods' advantages are easy preparation, effectively control of nucleation, preventing agglomeration, low viscosity, low energy consumption, thermodynamic stability, and reversible microemulsion formation. While the drawbacks of the microemulsion synthesis are the use of a large number of surfactants, pH and temperature affect the stability of the microemulsion, the limited dissolving capacity for substances with high melting points, and has low crystallinity due to slow nucleation rate at low temperature resulting in low yields ([Kefeni et al., 2017](#); [Sharifianjazi et al., 2020](#); [Simonazzi et al., 2018](#)). The synthesis schematic of several magnetic materials via the microemulsion method can be seen in [Figs. 5–7](#).

2.6. Microwave-assisted synthesis

Synthesis of magnetic nanomaterials, classifications and its applications by microwave-assisted method have been presented in the literature [Table 7](#). At present, synthesis of multi-purpose material has widely used microwave-assisted heating methods to increase the reaction rate and good control of the magnetic nanoparticles formation ([Kefeni et al., 2017](#)). In the synthesis of magnetic nanoparticles by microwave-assisted method, electromagnetic irradiation occurs through ionic conduction and molecular motion of precursor solvents

and reducing agents. Thermal energy will be generated from this process as the conversion form from electromagnetic energy ([Bolade et al., 2020](#)). Generally, the sample irradiation process exerts the temperature of $100\text{--}200^\circ\text{C}$ with fast reaction time ([Gonzalez-Moragas et al., 2015](#)).

Compared to conventional heating methods, microwave-assisted synthesis is based on efficient heating of the sample by dielectric heating effect. Dielectric heating in the sample works by two main mechanisms, namely dipolar polarization and ion conduction which will induce electrons in the sample, and then convert them into kinetic energy which is ultimately converted into heat ([Morsali et al., 2020](#)). Furthermore, the major advantages of microwave-assisted synthesis are increased uniform reaction rate, high reproducibility, high yield and purity of product, lower processing cost, small and narrow particle size distribution, and energy saving compared to other conventional approaches. While this method has major limitations, namely the type of vessel/reactor used and in-situ temperature measurement ([Gupta et al., 2018](#)). [Mahmoud et al. \(2016\)](#) synthesized a functionalized nanomagnetic iron oxide with 3-aminopropyltriethoxysilane [$\text{Nano-Fe}_3\text{O}_4\text{-SiO}_2\text{-NH}_2$] through microwave-assisted heating method for heavy metals ions extraction from aqueous solution. The results of microwave-assisted adsorption revealed that the maximum adsorption capacity of Cu (II), Cd (II) and Hg (II) was 1050 , 350 and $350\ \mu\text{mol.g}^{-1}$ after 25, 15 and 25 s heating periods, respectively. In addition, the microwave-assisted adsorption method exhibited the excellent performance in the process of extracting heavy metal ions in aqueous solution.

Table 7 The list of some commonly used magnetic source for producing iron-based nanocomposites by Microwave-assisted methods.

Magnetic Source	Modifier	Solvent	Reaction Temperature (°C)	Microwave Power (Watt)	Reaction Period	Particle Size (nm)	Magnetic Saturation Value (emu.g ⁻¹)	Iron Form	Application	Classification	Ref.
Fe(acac) ₃	Oleic acid	Benzyl alcohol	205	800	30 min	5–7	97–98	Magnetite	Magnetic fluid hyperthermia	Metal Oxide-based Material	(Kostyukhin and Kustov, 2018)
FeCl ₃ , FeCl ₂	Sm ³⁺	Ethylene Glycol, PEG	200	300	180 min	~ 4.5	33	Maghemite	Biomedicine	Metal Oxide-based Material	(Lastovina et al., 2018)
FeCl ₃ ·6H ₂ O, FeCl ₂ ·4H ₂ O	Zn ²⁺ , Ag ⁺ , Br ⁻	Ethanol, Water	NA	550	10 min	~ 200	3.31	Magnetite	Antifungal	Metal Oxide-based Material	(Hoseinzadeh et al., 2016)
Fe(acac) ₃	Trisodium citrate dihydrate	Benzyl alcohol	180–210	300–500	~ 8 min	~ 4–6	62	Hematite and Maghemite	NA	Metal Oxide-based Material	(Gonzalez-Moragas et al., 2015)
Fe(NO ₃) ₃ ·9H ₂ O	Citric acid	Water	NA	750	2 min	25–30	28.8–86.5	Magnetite	NA	Metal Oxide-based Material	(Radpour et al., 2017)
Fe(acac) ₃	Oleic acid, Oleylamine	Ethylene Glycol, Isooctane	230–300	850	15–30 min	4, 20.50 and 200	42–95	Magnetite	NA	Metal Oxide-based Material	(Liang et al., 2017)
Fe ₂ (SO ₄) ₃	Sodium acetate	Ethylene Glycol, PEG	200	300	10 min	52	58	Magnetite	Hyperthermia application	Metal Oxide-based Material	(Sathya et al., 2017)
FeCl ₃ ·6H ₂ O, FeCl ₂ ·4H ₂ O	Zr ⁴⁺	Water	RT	100–900	100 min	35	~ 2	Magnetite	Antimicrobial in dental filler	Metal Oxide-based Material	(Imran et al., 2019)
Fe(acac) ₃	Pectin, β-isopropylglutaric acid	Water, Acetic acid, Oleic acid, Oleylamine	185	100	30 min	4.3	50.1	Magnetite	Adsorption of dye	Metal Oxide-based Material	(Rakhshae and Noorani, 2017)
Fe(acac) ₃ , Co(acac) ₃	NA	Ethanol	150	800	180 min	10	NA	Magnetite	Acetone sensor	Metal Oxide-based Material	(Zhang et al., 2019)
FeCl ₃ ·6H ₂ O	Zn ²⁺ , TEOS, Trisodium citrate dihydrate	Water, Ethylene Glycol, Diethylene Glycol (DEG)	160	NA	15–60 min	~ 500	~ 18–80	Magnetite	Photocatalytic degradation	Metal Oxide-based Material	(Liu et al., 2019)
Fe(C ₅ H ₅) ₂ , FeCl ₃	NA	Ethanol, Acetonitrile	NA	800	1.5 min	5–10	30.4	Magnetite	NA	Carbon-based Material	(Kumar et al., 2017)
FeCl ₃ ·6H ₂ O	Graphene Oxide, Oleic acid	Benzyl alcohol	176	300	10 min	2–8	~ 5–15	Magnetite and Maghemite	NA	Reduced Graphene Oxide-Based Material	(Bertran et al., 2020)
Fe(C ₅ H ₅) ₂	Graphite Oxide Powder	Ethanol	NA	700	1.75 min	≤ 400	NA	Magnetite	High performance Lithium batteries	Reduced Graphene Oxide-Based Material	(Kumar et al., 2018)
FeCl ₃ ·6H ₂ O	NaAc, H ₃ BTC	Water, Ethylene Glycol	150	300	30 min	~ 200	15.1	Magnetite	Adsorbent and Photocatalyst	MOFs-Based Material	(Li et al., 2019)
FeCl ₃ ·6H ₂ O, FeCl ₂ ·4H ₂ O	SDS, DVB, Acrylic Acid, KPS and PVP40	Water, Ethylene Glycol, PEG-200	200 and 80	900	30 min	25–33	22.5	Magnetite	Biomedical, catalysis and Magnetic sensor	Polymer-Based Material	(Jaiswal et al., 2018)
FeCl ₃ ·6H ₂ O	Mg ²⁺ , TEOS, Ammonia chloride	Water, Ethanol, Ethylene Glycol, PEG200	160	NA	30 min	~ 615	66.5	Magnetite	Adsorption of heavy metal ions	Silica-Based Material	(Zhao et al., 2017)
FeCl ₃ , FeCl ₂	HCl, NaOH, Sodium silicate, APTES	Water	80	1400	~ 12 min	~ 4–9	NA	Magnetite	Adsorption of heavy metal ions	Silica-Based Material	(Mahmoud et al., 2016)

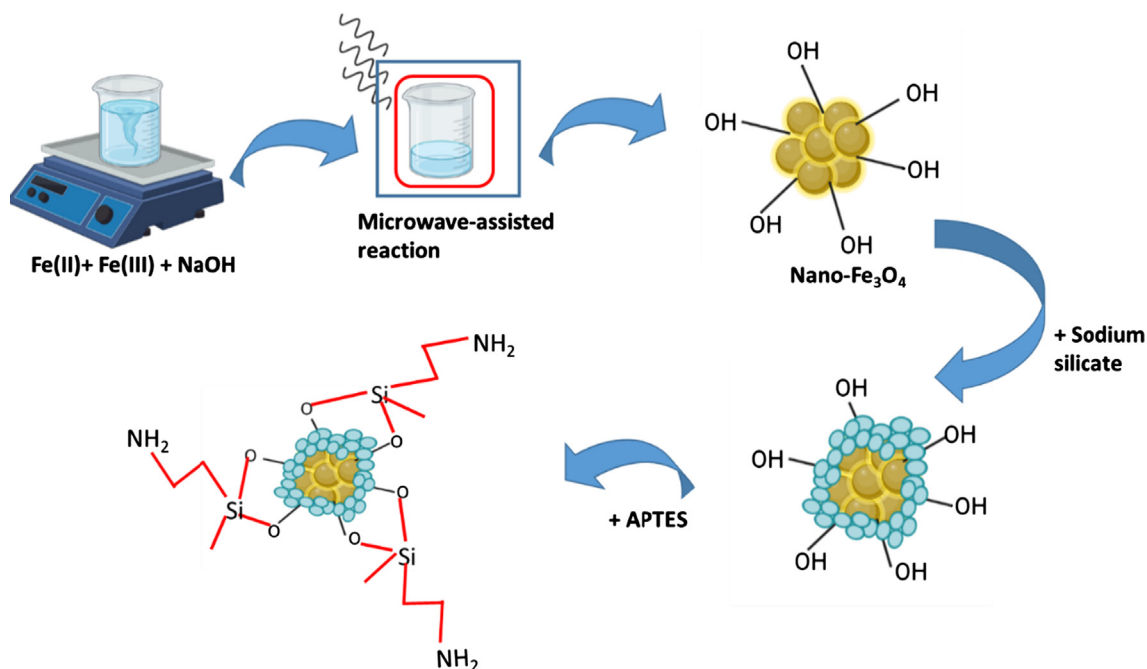


Fig. 8 Illustration of microwave-assisted synthesis of Nano-Fe₃O₄-SiO₂-NH₂ adsorbent (Singh and Upadhyay, 2018).

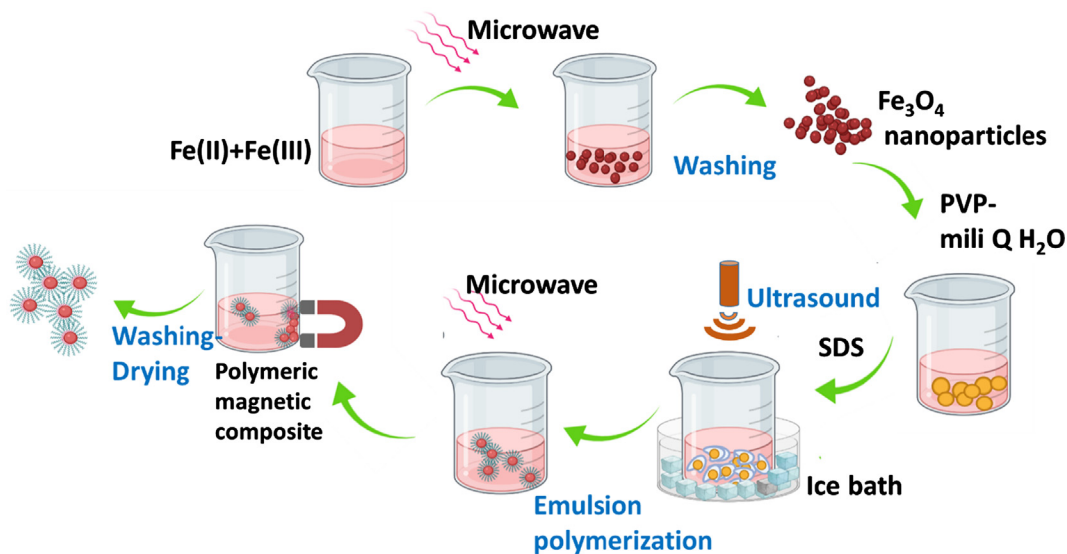


Fig. 9 Schematic of the microwave-assisted synthesis of Fe₃O₄ nanoparticles and Fe₃O₄/poly(styrene-divinylbenzene-acrylic acid) composites by Jaiswal et al. (2018).

Jaiswal et al. (2018) reported the rapid synthesis of highly crystalline superparamagnetic Fe₃O₄ nanoparticles via microwave-assisted method. The obtained Fe₃O₄ nanoparticles have the crystallite size of 25 to 33 nm. Furthermore, the synthesis of spherical polymers magnetic composite (PMCs) from PVP-stabilized Fe₃O₄, is carried out through microwave-irradiated emulsion polymerization using vinyl monomers. The characterization results indicated that the superparamagnetic Fe₃O₄ nanoparticles were integrated in a cross-linked polymer matrix (styrene-divinylbenzene-acrylic acid). The

obtained Fe₃O₄ nanoparticles revealed superparamagnetic properties at 300 K with the saturation magnetization of 67.5 emu.g⁻¹. Whereas the synthesized responsive magnetic PMC [Fe₃O₄/P(St-DVB-AA)] showed ferromagnetic properties at temperature intervals of 10–350 K which were different from the synthesized Fe₃O₄.

While Kumar et al. (2017) exhibited the large-scale synthesis of octahedral iron oxide nanocrystals (Fe₃O₄-ONCs) embedded on the reduced graphene oxide nanosheets (rGO NSs), (Fe₃O₄-ONCs@rGO hybrids) via microwave-assisted

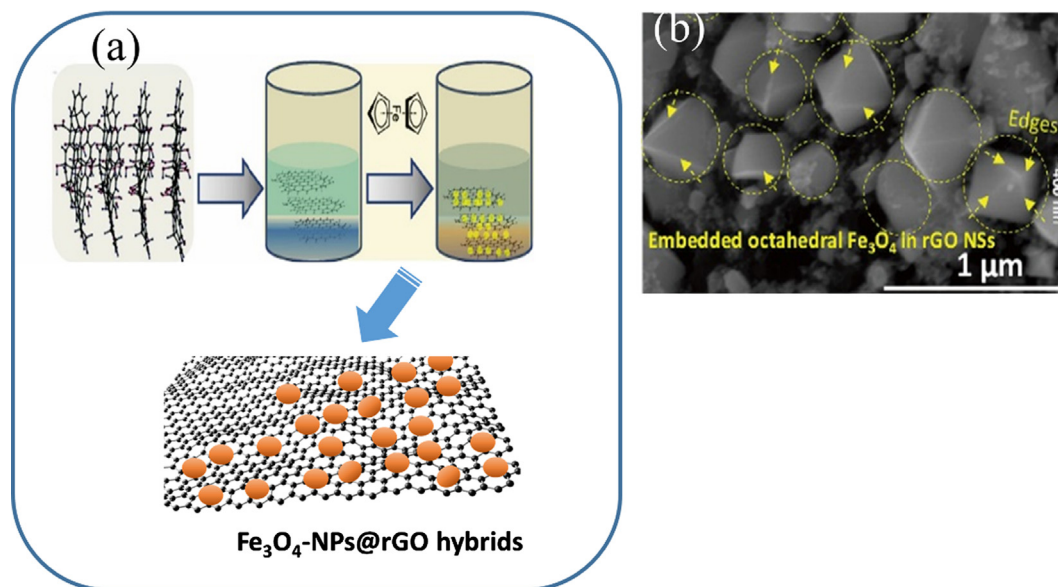


Fig. 10 (a) The synthesis schematic of $\text{Fe}_3\text{O}_4\text{-NPs@rGO}$ hybrids by Kumar et al. (2018); (b) SEM $\text{Fe}_3\text{O}_4\text{-ONCs@rGO}$ hybrids.

method. During the synthesis process, rGO NSs provide a structural board to implant positively charged $\text{Fe}_3\text{O}_4\text{-ONCs}$ using the electrostatic assembly followed by the microwave reduction of rGO NSs. Experimental results indicated that $\text{Fe}_3\text{O}_4\text{-ONCs@rGO}$ hybrids shows superior electrochemical performance better than $\text{Fe}_3\text{O}_4\text{-NPs@rGO}$, including better cycling stability and performance value, which may be affected by the embedded nano-size $\text{Fe}_3\text{O}_4\text{-ONCs}$ in rGO NSs. Furthermore, this low-cost and fast synthesis method can be used in other structured hybrids for high-performance lithium batteries. The synthesis schematic of several magnetic materials via the microwave-assisted synthesis method can be seen in Figs. 8–10.

3. Future perspective

This review has summarized and highlighted several methods for synthesizing iron oxide nanocomposites, such as co-precipitation, chemical vapor deposition (CVD), electrochemical method, solvothermal, microwave, and micro-emulsion. Generally, the stability of the precursor material plays an essential role in the quantity of nanoparticles produced. In addition, several factors such as pH, temperature, supporting electrolyte, salts, etc., directly influence. The magnetic characteristics of the iron nanocomposite material are determined by the natural type of iron oxide itself. However, monitoring temperature during a process is crucial because the iron oxide can change the phase during the synthesis. Several routes of the synthesis of magnetic iron oxide nanocomposites have been well studied. Review presents the incorporating functional magnetic nanoparticles into the nanocomposite structures by different method with various nanoparticle size and saturation magnetization for such applications. The intensification of the synthesis for fast and greener method consist of microwave-assisted method was also addressed. Thus, we have recommended that researcher's study large scale production and implementation, including the following:

- Modeling of synthesis procedure by simulating several factors influence on the performance of nanocomposite for applicability in industrial scale.
- Life cycle assessment on the synthesis method should be given to minimize chemical waste during synthesis.

Declaration of Competing Interest

The authors declare that they have no known competing financial interests or personal relationships that could have appeared to influence the work reported in this paper.

Acknowledgement

The research has been funded by Chemistry Department, Universitas Islam Indonesia by Research Excellencies Support 2021.

References

- Ait Kerroum, M.A., Essyed, A., Iacovita, C., Baaziz, W., Ihi-awakrim, D., Mounkachi, O., Hamedoun, M., Benyoussef, A., Benaissa, M., Ersen, O., 2019. The effect of basic pH on the elaboration of ZnFe_2O_4 nanoparticles by co-precipitation method: Structural, magnetic and hyperthermia characterization. *J. Magn. Mater.* 478, 239–246. <https://doi.org/10.1016/j.jmmm.2019.01.081>.
- Alijani, H., Beyki, M.H., Shariatnia, Z., Bayat, M., Shemirani, F., 2014. A new approach for one step synthesis of magnetic carbon nanotubes/diatomite earth composite by chemical vapor deposition method: Application for removal of lead ions. *Chem. Eng. J.* 253, 456–463. <https://doi.org/10.1016/j.cej.2014.05.021>.
- Andrade Neto, N.F., Nascimento, L.E., Correa, M., Bohn, F., Bomio, M.R.D., Motta, F.V., 2020. Characterization and photocatalytic application of Ce^{4+} , Co^{2+} , Mn^{2+} and Ni^{2+} doped Fe_3O_4 magnetic nanoparticles obtained by the co-precipitation method. *Mater. Chem. Phys.* 242, <https://doi.org/10.1016/j.matchemphys.2019.122489> 122489.

- Ansari, N., Payami, Z., Feghhi, F., 2020. Synthesis of iron/graphene composites with controlled magnetization by electrochemical exfoliation/deposition using sodium dodecyl sulfate as surfactant. *J. Magn. Magn. Mater.* 500,. <https://doi.org/10.1016/j.jmmm.2020.166398> 166398.
- Asgari, M., Soleymani, M., Miri, T., Barati, A., 2019. A robust method for fabrication of monodisperse magnetic mesoporous silica nanoparticles with core-shell structure as anticancer drug carriers. *J. Mol. Liq.* 292,. <https://doi.org/10.1016/j.molliq.2019.111367> 111367.
- Atchudan, R., Jebakumar Immanuel Edison, T.N., Perumal, S., RanjithKumar, D., Lee, Y.R., 2019. Direct growth of iron oxide nanoparticles filled multi-walled carbon nanotube via chemical vapour deposition method as high-performance supercapacitors. *Int. J. Hydrogen Energy* 44, 2349–2360. <https://doi.org/10.1016/j.ijhydene.2018.08.183>.
- Bertran, A., Sandoval, S., Oró-Solé, J., Sánchez, À., Tobias, G., 2020. Particle size determination from magnetization curves in reduced graphene oxide decorated with monodispersed superparamagnetic iron oxide nanoparticles. *J. Colloid Interface Sci.* 566, 107–119. <https://doi.org/10.1016/j.jcis.2020.01.072>.
- Beygi, H., Babakhani, A., 2017. Microemulsion synthesis and magnetic properties of Fe_xNi(1-x) alloy nanoparticles. *J. Magn. Magn. Mater.* 421, 177–183. <https://doi.org/10.1016/j.jmmm.2016.07.071>.
- Bolade, O.P., Williams, A.B., Benson, N.U., 2020. Green synthesis of iron-based nanomaterials for environmental remediation: A review. *Environ. Nanotechnol. Monit. Manage.* 13,. <https://doi.org/10.1016/j.enmm.2019.100279> 100279.
- Cao, J., Chang, G., Guo, H., Chen, J., 2013. Synthesis and characterization of magnetic ZSM-5 zeolite. *Trans. Tianjin Univ.* 19, 326–331. <https://doi.org/10.1007/s12209-013-1912-0>.
- Cardoso, V., Francesko, A., Ribeiro, C., Bañobre-López, M., Martins, P., Lanceros-Méndez, S., 2017. Advances in Magnetic Nanoparticles for Biomedical Applications. *Adv. Healthcare Mater.* 7, 1700845. <https://doi.org/10.1002/adhm.201700845>.
- Chandra, S., Mehta, S., Nigam, S., Bahadur, D., 2010. Dendritic magnetite nanocarriers for drug delivery applications. *New J. Chem.* 34, 648–655. <https://doi.org/10.1039/B9NJ00609E>.
- Chandrika, M., Ravindra, A.V., Rajesh, C., Ramarao, S.D., Ju, S., 2019. Studies on structural and optical properties of nano ZnFe₂O₄ and ZnFe₂O₄-TiO₂ composite synthesized by co-precipitation route. *Mater. Chem. Phys.* 230, 107–113. <https://doi.org/10.1016/j.matchemphys.2019.03.059>.
- Chávez, A.M., Solís, R.R., Beltrán, F.J., 2020. Magnetic graphene TiO₂-based photocatalyst for the removal of pollutants of emerging concern in water by simulated sunlight aided photocatalytic ozonation. *Appl. Catal. B* 262,. <https://doi.org/10.1016/j.apcatb.2019.118275> 118275.
- Chen, L., Li, Z., Li, G., Zhou, M., He, B., Ouyang, J., Xu, W., Wang, W., Hou, Z., 2020. A facile self-catalyzed CVD method to synthesize Fe₃C/N-doped carbon nanofibers as lithium storage anode with improved rate capability and cyclability. *J. Mater. Sci. Technol.* 44, 229–236. <https://doi.org/10.1016/j.jmst.2019.11.013>.
- Chu, H., Hu, X., Yao, J., Yan, G., Sun, N., Deng, C., 2020. One-pot preparation of hydrophilic citric acid-magnetic nanoparticles for identification of glycopeptides in human saliva. *Talanta* 206,. <https://doi.org/10.1016/j.talanta.2019.120178> 120178.
- Cui, Y., Qin, L., Kang, W., Ma, J., Yang, Y., Liu, X., 2020. Magnetic carbon nanospheres: Synthesis, characterization, and adsorbability towards quinoline from coking wastewater. *Chem. Eng. J.* 382,. <https://doi.org/10.1016/j.cej.2019.122995> 122995.
- de Mello, L.B., Varanda, L.C., Sigoli, F.A., Mazali, I.O., 2019. Co-precipitation synthesis of (Zn-Mn)-co-doped magnetite nanoparticles and their application in magnetic hyperthermia. *J. Alloy. Compd.* 779, 698–705. <https://doi.org/10.1016/j.jallcom.2018.11.280>.
- Dhand, V., Mittal, G., Rhee, K.Y., Park, S.-J., 2017. Synthesis and comparison of different spinel ferrites and their catalytic activity during chemical vapor deposition of polymorphic nanocarbons. *Int. J. Precis. Eng. Manuf.-Green Technol.* 4, 441–451. <https://doi.org/10.1007/s40684-017-0049-3>.
- Dung, C.T., Quynh, L.M., Linh, N.P., Nam, N.H., Luong, N.H., 2016. Synthesis of ZnS:Mn-Fe₃O₄ bifunctional nanoparticles by inverse microemulsion method. *J. Sci.: Adv. Mater. Devices* 1, 200–203. <https://doi.org/10.1016/j.jsamd.2016.06.006>.
- Elaïssari, A., Bourrel, V., 2001. Thermosensitive magnetic latex particles for controlling protein adsorption and desorption. *J. Magn. Magn. Mater.* 225, 151–155. [https://doi.org/10.1016/S0304-8853\(00\)01244-0](https://doi.org/10.1016/S0304-8853(00)01244-0).
- Elrouby, M., Abdel-Mawgoud, A.M., El-Rahman, R.A., 2017. Synthesis of iron oxides nanoparticles with very high saturation magnetization form TEA-Fe(III) complex via electrochemical deposition for supercapacitor applications. *J. Mol. Struct.* 1147, 84–95. <https://doi.org/10.1016/j.molstruc.2017.06.092>.
- Erdemi, H., Baykal, A., 2015. Dielectric properties of triethylene glycol-stabilized Mn_{1-x}Zn_xFe₂O₄ nanoparticles. *Mater. Chem. Phys.* 165, 156–167. <https://doi.org/10.1016/j.matchemphys.2015.09.011>.
- Fayazi, M., Taher, M.A., Afzali, D., Mostafavi, A., 2016. Fe₃O₄ and MnO₂ assembled on halloysite nanotubes: A highly efficient solid-phase extractant for electrochemical detection of mercury(II) ions. *Sens. Actuators, B* 228, 1–9. <https://doi.org/10.1016/j.snb.2015.12.107>.
- Feng, S.H., Li, G.H., 2017. Chapter 4 - Hydrothermal and Solvothermal Syntheses. In: Xu, R., Xu, Y. (Eds.), *Modern Inorganic Synthetic Chemistry*. second ed. Elsevier, Amsterdam, pp. 73–104.
- Foroughi, F., Hassanzadeh-Tabrizi, S.A., Bigham, A., 2016. In situ microemulsion synthesis of hydroxyapatite-MgFe₂O₄ nanocomposite as a magnetic drug delivery system. *Mater. Sci. Eng., C* 68, 774–779. <https://doi.org/10.1016/j.msec.2016.07.028>.
- Fotukian, S.M., Barati, A., Soleymani, M., Alizadeh, A.M., 2020. Solvothermal synthesis of CuFe₂O₄ and Fe₃O₄ nanoparticles with high heating efficiency for magnetic hyperthermia application. *J. Alloy. Compd.* 816,. <https://doi.org/10.1016/j.jallcom.2019.152548> 152548.
- Gnanaprakash, G., Mahadevan, S., Jayakumar, T., Kalyanasundaram, P., Philip, J., Raj, B., 2007. Effect of initial pH and temperature of iron salt solutions on formation of magnetite nanoparticles. *Mater. Chem. Phys.*, 168–175 <https://doi.org/10.1016/j.matchemphys.2007.02.011>.
- Gonzalez-Moragas, L., Yu, S.-M., Murillo-Cremaes, N., Laromaine, A., Roig, A., 2015. Scale-up synthesis of iron oxide nanoparticles by microwave-assisted thermal decomposition. *Chem. Eng. J.* 281, 87–95. <https://doi.org/10.1016/j.cej.2015.06.066>.
- Gupta, D., Jamwal, D., Rana, D., Katoch, A., 2018. 26 - Microwave synthesized nanocomposites for enhancing oral bioavailability of drugs. In: Inamuddin, Asiri, A.M., Mohammad, A. (Eds.), *Applications of Nanocomposite Materials in Drug Delivery*. Woodhead Publishing, pp. 619–632.
- Haramagatti, C.R., Dhande, P., Bhavsar, R., Umbarkar, A., Joshi, A., 2018. Role of surfactants on stability of iron oxide yellow pigment dispersions. *Prog. Org. Coat.* 120, 260–265. <https://doi.org/10.1016/j.porgcoat.2018.03.006>.
- Hoseinzadeh, A., Habibi-Yangjeh, A., Davari, M., 2016. Antifungal activity of magnetically separable Fe₃O₄/ZnO/AgBr nanocomposites prepared by a facile microwave-assisted method. *Progr. Nat. Sci. Mater. Int.* 26, 334–340. <https://doi.org/10.1016/j.pnsc.2016.06.006>.
- Huang, Q., Chen, Y., Yu, H., Yan, L., Zhang, J., Wang, B., Du, B., Xing, L., 2018. Magnetic graphene oxide/MgAl-layered double hydroxide nanocomposite: One-pot solvothermal synthesis, adsorption performance and mechanisms for Pb²⁺, Cd²⁺, and Cu²⁺. *Chem. Eng. J.* 341, 1–9. <https://doi.org/10.1016/j.cej.2018.01.156>.

- Huang, X., Liu, L., Xi, Z., Zheng, H., Dong, W., Wang, G., 2019. One-pot solvothermal synthesis of magnetically separable rGO/MnFe₂O₄ hybrids as efficient photocatalysts for degradation of MB under visible light. *Mater. Chem. Phys.* 231, 68–74. <https://doi.org/10.1016/j.matchemphys.2019.03.076>.
- Imran, M., Riaz, S., Sanaullah, I., Khan, U., Sabri, A.N., Naseem, S., 2019. Microwave assisted synthesis and antimicrobial activity of Fe₃O₄-doped ZrO₂ nanoparticles. *Ceram. Int.* 45, 10106–10113. <https://doi.org/10.1016/j.ceramint.2019.02.057>.
- Irawan, C., Nata, I.F., Lee, C.-K., 2019. Removal of Pb(II) and As (V) using magnetic nanoparticles coated montmorillonite via one-pot solvothermal reaction as adsorbent. *J. Environ. Chem. Eng.* 7, <https://doi.org/10.1016/j.jece.2019.103000> 103000.
- Jaiswal, K.K., Manikandan, D., Murugan, R., Ramaswamy, A.P., 2018. Microwave-assisted rapid synthesis of Fe₃O₄/poly(styrene-divinylbenzene-acrylic acid) polymeric magnetic composites and investigation of their structural and magnetic properties. *Eur. Polym. J.* 98, 177–190. <https://doi.org/10.1016/j.eurpolymj.2017.11.005>.
- Jesus, A.C.B., Jesus, J.R., Lima, R.J.S., Moura, K.O., Almeida, J.M.A., Duque, J.G.S., Meneses, C.T., 2020. Synthesis and magnetic interaction on concentrated Fe₃O₄ nanoparticles obtained by the co-precipitation and hydrothermal chemical methods. *Ceram. Int.* 46, 11149–11153. <https://doi.org/10.1016/j.ceramint.2020.01.135>.
- Jia, H., Huang, F., Gao, Z., Zhong, C., Zhou, H., Jiang, M., Wei, P., 2016. Immobilization of ω -transaminase by magnetic PVA-Fe₃O₄ nanoparticles. *Biotechnol. Rep.* 10, 49–55. <https://doi.org/10.1016/j.btre.2016.03.004>.
- Jun, L., Ying, L., Jing, G., Xiaoxi, Z., Yilong, M., 2013. Microstructure and magnetic properties of bulk Nd₂Fe₁₄B/ α -Fe nanocomposite prepared by chemical vapor deposition. *J. Magn. Magn. Mater.* 328, 1–6. <https://doi.org/10.1016/j.jmmm.2012.09.050>.
- Kaewmanee, T., Phuruangrat, A., Thongtem, T., Thongtem, S., 2020. Solvothermal synthesis of Mn–Zn Ferrite(core)@SiO₂(shell)/BiOBr 0.5Cl_{0.5} nanocomposites used for adsorption and photocatalysis combination. *Ceram. Int.* 46, 3655–3662. <https://doi.org/10.1016/j.ceramint.2019.10.085>.
- Karimzadeh, I., Dizaji, H.R., Aghazadeh, M., 2016. Development of a facile and effective electrochemical strategy for preparation of iron oxides (Fe₃O₄ and γ -Fe₂O₃) nanoparticles from aqueous and ethanol mediums and in situ PVC coating of Fe₃O₄ superparamagnetic nanoparticles for biomedical applications. *J. Magn. Magn. Mater.* 416, 81–88. <https://doi.org/10.1016/j.jmmm.2016.05.015>.
- Karthikeyan, P., Vigneshwaran, S., Preethi, J., Meenakshi, S., 2020. Preparation of novel cobalt ferrite coated-porous carbon composite by simple chemical co-precipitation method and their mechanistic performance. *Diam. Relat. Mater.* 108, <https://doi.org/10.1016/j.diamond.2020.107922> 107922.
- Kefeni, K.K., Msagati, T.A.M., Mamba, B.B., 2017. Ferrite nanoparticles: Synthesis, characterisation and applications in electronic device. *Mater. Sci. Eng., B* 215, 37–55. <https://doi.org/10.1016/j.mseb.2016.11.002>.
- Klencsár, Z., Ábrahám, A., Szabó, L., Szabó, E.G., Stichleutner, S., Kuzmann, E., Homonnay, Z., Tolnai, G., 2019. The effect of preparation conditions on magnetite nanoparticles obtained via chemical co-precipitation. *Mater. Chem. Phys.* 223, 122–132. <https://doi.org/10.1016/j.matchemphys.2018.10.049>.
- Kostyukhin, E.M., Kustov, L.M., 2018. Microwave-assisted synthesis of magnetite nanoparticles possessing superior magnetic properties. *Mendelevov Commun.* 28, 559–561. <https://doi.org/10.1016/j.mencom.2018.09.038>.
- Kumar, R., Singh, R.K., Tiwari, V.S., Yadav, A., Savu, R., Vaz, A.R., Moshkalev, S.A., 2017. Enhanced magnetic performance of iron oxide nanoparticles anchored pristine/ N-doped multi-walled carbon nanotubes by microwave-assisted approach. *J. Alloy. Compd.* 695, 1793–1801. <https://doi.org/10.1016/j.jallcom.2016.11.010>.
- Kumar, R., Singh, R.K., Alaferdov, A.V., Moshkalev, S.A., 2018. Rapid and controllable synthesis of Fe₃O₄ octahedral nanocrystals embedded-reduced graphene oxide using microwave irradiation for high performance lithium-ion batteries. *Electrochim. Acta* 281, 78–87. <https://doi.org/10.1016/j.electacta.2018.05.157>.
- Ladj, R., Bitar, A., Eissa, M., Mugnier, Y., Le Dantec, R., Fessi, H., Elaissari, A., 2013. Individual inorganic nanoparticles: preparation, functionalization and in vitro biomedical diagnostic applications. *J. Mater. Chem. B* 1, 1381–1396. <https://doi.org/10.1039/C2TB00301E>.
- Lassalle, V.L., Zysler, R.D., Ferreira, M.L., 2011. Novel and facile synthesis of magnetic composites by a modified co-precipitation method. *Mater. Chem. Phys.* 130, 624–634. <https://doi.org/10.1016/j.matchemphys.2011.07.035>.
- Lastovina, T.A., Budnyk, A.P., Kubrin, S.P., Soldatov, A.V., 2018. Microwave-assisted synthesis of ultra-small iron oxide nanoparticles for biomedicine. *Mendelevov Commun.* 28, 167–169. <https://doi.org/10.1016/j.mencom.2018.03.019>.
- Lee, J.-S., Song, Y.-J., Hsu, H.-S., Lin, C.-R., Huang, J.-Y., Chen, J., 2019. Magnetic enhancement of carbon-encapsulated magnetite nanoparticles. *J. Alloy. Compd.* 790, 716–722. <https://doi.org/10.1016/j.jallcom.2019.03.191>.
- Li, S., Cui, J., Wu, X., Zhang, X., Hu, Q., Hou, X., 2019. Rapid in situ microwave synthesis of Fe₃O₄@MIL-100(Fe) for aqueous diclofenac sodium removal through integrated adsorption and photodegradation. *J. Hazard. Mater.* 373, 408–416. <https://doi.org/10.1016/j.jhazmat.2019.03.102>.
- Li, Y., Hu, K., Chen, B., Liang, Y., Fan, F., Sun, J., Zhang, Y., Gu, N., 2017. Fe₃O₄@PSC nanoparticle clusters with enhanced magnetic properties prepared by alternating-current magnetic field assisted co-precipitation. *Colloids Surf., A* 520, 348–354. <https://doi.org/10.1016/j.colsurfa.2017.01.073>.
- Li, Q., Kartikowati, C.W., Horie, S., Ogi, T., Iwaki, T., Okuyama, K., 2017. Correlation between particle size/domain structure and magnetic properties of highly crystalline Fe₃O₄ nanoparticles. *Sci. Rep.* 7, 9894. <https://doi.org/10.1038/s41598-017-09897-5>.
- Li, Y., Peng, S.J., Zhang, M., Wang, S.H., Zhu, S.C., Zhang, J.E., Shen, F.R., 2019. Magnetic properties and microstructure of nanocomposite (La, Pr)₃Fe₁₄B ribbons by doping La element. *AIP Adv.* 9, <https://doi.org/10.1063/1.5079848> 035111.
- Liang, Y.-J., Fan, F., Ma, M., Sun, J., Chen, J., Zhang, Y., Gu, N., 2017. Size-dependent electromagnetic properties and the related simulations of Fe₃O₄ nanoparticles made by microwave-assisted thermal decomposition. *Colloids Surf., A* 530, 191–199. <https://doi.org/10.1016/j.colsurfa.2017.06.059>.
- Liao, W., Ma, Y., Chen, A., Yang, Y., 2015. Preparation of fatty acids coated Fe₃O₄ nanoparticles for adsorption and determination of benzo(a)pyrene in environmental water samples. *Chem. Eng. J.* 271, 232–239. <https://doi.org/10.1016/j.cej.2015.03.010>.
- Lin, J., Wen, Q., Chen, S., Le, X., Zhou, X., Huang, L., 2017. Synthesis of amine-functionalized Fe₃O₄@C nanoparticles for lactase immobilization. *Int. J. Biol. Macromol.* 96, 377–383. <https://doi.org/10.1016/j.ijbiomac.2016.12.051>.
- Liu, T., Liu, N., Zhai, S., Gao, S., Xiao, Z., An, Q., Yang, D., 2019. Tailor-made core/shell/shell-like Fe₃O₄@SiO₂@PPy composites with prominent microwave absorption performance. *J. Alloy. Compd.* 779, 831–843. <https://doi.org/10.1016/j.jallcom.2018.11.167>.
- Liu, S., Ma, C., Ma, M.-G., Xu, F., 2019. 12 - Magnetic Nanocomposite Adsorbents. In: Kyzas, G.Z., Mitropoulos, A.C. (Eds.), *Composite Nanoadsorbents*. Elsevier, pp. 295–316.
- Liu, K., Qin, Y., Muhammad, Y., Zhu, Y., Tang, R., Chen, N., Shi, H., Zhang, H., Tong, Z., Yu, B., 2019. Effect of Fe₃O₄ content and microwave reaction time on the properties of Fe₃O₄/ZnO magnetic nanoparticles. *J. Alloy. Compd.* 781, 790–799. <https://doi.org/10.1016/j.jallcom.2018.12.085>.

- Liu, X., Zhang, S., Luo, H., Zhang, Y., Xu, Q., Zhang, Z., Xu, H., Wang, Z., 2017. Biomass activated carbon supported with high crystallinity and dispersion Fe₃O₄ nanoparticle for preconcentration and effective degradation of methylene blue. *J. Taiwan Inst. Chem. Eng.* 81, 265–274. <https://doi.org/10.1016/j.jtice.2017.10.002>.
- Lopez, D., Abe, I.Y., Pereyra, I., 2015. Temperature effect on the synthesis of carbon nanotubes and core-shell Ni nanoparticle by thermal CVD. *Diam. Relat. Mater.* 52, 59–65. <https://doi.org/10.1016/j.diamond.2014.12.006>.
- Lucas-Granados, B., Sánchez-Tovar, R., Fernández-Domene, R.M., García-Antón, J., 2018. Influence of electrolyte temperature on the synthesis of iron oxide nanostructures by electrochemical anodization for water splitting. *Int. J. Hydrogen Energy* 43, 7923–7937. <https://doi.org/10.1016/j.ijhydene.2018.03.046>.
- Lv, H., Jiang, R., Li, Y., Zhang, X., Wang, J., 2015. Microemulsion-mediated hydrothermal growth of pagoda-like Fe₃O₄ microstructures and their application in a lithium-air battery. *Ceram. Int.* 41, 8843–8848. <https://doi.org/10.1016/j.ceramint.2015.03.114>.
- Maccato, C., Carraro, G., Peddis, D., Varvaro, G., Barreca, D., 2018. Magnetic properties of ϵ iron(III) oxide nanorod arrays functionalized with gold and copper(II) oxide. *Appl. Surf. Sci.* 427, 890–896. <https://doi.org/10.1016/j.apsusc.2017.09.015>.
- Mahmoud, M.E., Amira, M.F., Zaghoul, A.A., Ibrahim, G.A.A., 2016. Microwave-enforced sorption of heavy metals from aqueous solutions on the surface of magnetic iron oxide-functionalized-3-aminopropyltriethoxysilane. *Chem. Eng. J.* 293, 200–206. <https://doi.org/10.1016/j.cej.2016.02.056>.
- Majidi, S., Zeinali Sehrig, F., Farkhani, S.M., Soleymani Goloujeh, M., Akbarzadeh, A., 2016. Current methods for synthesis of magnetic nanoparticles. *Artif. Cells Nanomed. Biotechnol.* 44, 722–734. <https://doi.org/10.3109/21691401.2014.982802>.
- Marín, T., Montoya, P., Arnache, O., Calderón, J., 2016. Influence of Surface Treatment on Magnetic Properties of Fe₃O₄ Nanoparticles Synthesized by Electrochemical Method. *J. Phys. Chem. B* 120, 6634–6645. <https://doi.org/10.1021/acs.jpcc.6b01796>.
- Mascolo, M.C., Pei, Y., Ring, T.A., 2013. Room Temperature Co-Precipitation Synthesis of Magnetite Nanoparticles in a Large pH Window with Different Bases. *Materials (Basel)* 6, 5549–5567. <https://doi.org/10.3390/ma6125549>.
- Medeiros, S.F., Santos, A.M., Fessi, H., Elaissari, A., 2011. Stimuli-responsive magnetic particles for biomedical applications. *Int. J. Pharm.* 403, 139–161. <https://doi.org/10.1016/j.ijpharm.2010.10.011>.
- Meng, C., Zhikun, W., Qiang, L., Chunling, L., Shuangqing, S., Songqing, H., 2018. Preparation of amino-functionalized Fe₃O₄@mSiO₂ core-shell magnetic nanoparticles and their application for aqueous Fe³⁺ removal. *J. Hazard. Mater.* 341, 198–206. <https://doi.org/10.1016/j.jhazmat.2017.07.062>.
- Morsali, A., Hashemi, L., 2020. Chapter Two - Nanoscale coordination polymers: Preparation, function and application. In: Ruiz-Molina, D., van Eldik, R. (Eds.), *Advances in Inorganic Chemistry*. Academic Press, pp. 33–72.
- Mustaffa, M.S., Azis, R.A.S., Abdullah, N.H., Ismail, I., Ibrahim, I. R., 2019. An investigation of microstructural, magnetic and microwave absorption properties of multi-walled carbon nanotubes/Ni_{0.5}Zn_{0.5}Fe₂O₄. *Sci. Rep.* 9.
- Nguyen, T.A., Nguyen, L.T.T., Bui, V.X., Nguyen, D.H.T., Lieu, H. D., Le, L.M.T., Pham, V., 2020. Optical and magnetic properties of HoFeO₃ nanocrystals prepared by a simple co-precipitation method using ethanol. *J. Alloy. Compd.* 834. <https://doi.org/10.1016/j.jallcom.2020.155098> 155098.
- Nikolic, V.N., Spasojevic, V., Panjan, M., Kopanja, L., Mrakovic, A., Tadic, M., 2017. Re-formation of metastable ϵ -Fe₂O₃ in post-annealing of Fe₂O₃/SiO₂ nanostructure: Synthesis, computational particle shape analysis in micrographs and magnetic properties. *Ceram. Int.* 43, 7497–7507. <https://doi.org/10.1016/j.ceramint.2017.03.030>.
- Nunes, D., Pimentel, A., Santos, L., Barquinha, P., Pereira, L., Fortunato, E., Martins, R., 2019. 2 - Synthesis, design, and morphology of metal oxide nanostructures. In: Nunes, D., Pimentel, A., Santos, L., Barquinha, P., Pereira, L., Fortunato, E., Martins, R. (Eds.), *Metal Oxide Nanostructures*. Elsevier, NY, pp. 21–57.
- Ordóñez, F., Chejne, F., Pabón, E., Cacia, K., 2020. Synthesis of ZrO₂ nanoparticles and effect of surfactant on dispersion and stability. *Ceram. Int.* 46, 11970–11977. <https://doi.org/10.1016/j.ceramint.2020.01.236>.
- Peng, Y., Yi, Y., Li, L., Ai, H., Wang, X., Chen, L., 2017. Fe-based soft magnetic composites coated with NiZn ferrite prepared by a co-precipitation method. *J. Magn. Magn. Mater.* 428, 148–153. <https://doi.org/10.1016/j.jmmm.2016.12.024>.
- Qiao, K., Tian, W., Bai, J., Wang, L., Zhao, J., Du, Z., Gong, X., 2019. Application of magnetic adsorbents based on iron oxide nanoparticles for oil spill remediation: A review. *J. Taiwan Inst. Chem. Eng.* 97, 227–236. <https://doi.org/10.1016/j.jtice.2019.01.029>.
- Qin, H., Cheng, H., Li, H., Wang, Y., 2020. Degradation of ofloxacin, amoxicillin and tetracycline antibiotics using magnetic core-shell MnFe₂O₄@C-NH₂ as a heterogeneous Fenton catalyst. *Chem. Eng. J.* 396. <https://doi.org/10.1016/j.cej.2020.125304> 125304.
- Radoń, A., Kubacki, J., Kądziołka-Gawel, M., Gębara, P., Hawelek, Ł., Topolska, S., Łukowiec, D., 2020. Structure and magnetic properties of ultrafine superparamagnetic Sn-doped magnetite nanoparticles synthesized by glycol assisted co-precipitation method. *J. Phys. Chem. Solids* 145. <https://doi.org/10.1016/j.jpcs.2020.109530> 109530.
- Radpour, M., Masoudpanah, S.M., Alamolhoda, S., 2017. Microwave-assisted solution combustion synthesis of Fe₃O₄ powders. *Ceram. Int.* 43, 14756–14762. <https://doi.org/10.1016/j.ceramint.2017.07.216>.
- Rakhshaei, R., Noorani, Y., 2017. Comparing three methods of simultaneous synthesis and stabilization of Fe₃O₄ nanoparticles: Changing physicochemical properties of products to improve kinetic and thermodynamic of dye adsorption. *J. Magn. Magn. Mater.* 422, 128–140. <https://doi.org/10.1016/j.jmmm.2016.08.078>.
- Ramimoghaddam, D., Bagheri, S., Hamid, S.B.A., 2014. Progress in electrochemical synthesis of magnetic iron oxide nanoparticles. *J. Magn. Magn. Mater.* 368, 207–229. <https://doi.org/10.1016/j.jmmm.2014.05.015>.
- Rane, A.V., Kanny, K., Abitha, V.K., Thomas, S., 2018. Chapter 5 - Methods for Synthesis of Nanoparticles and Fabrication of Nanocomposites. In: MohanBhagyaraj, S., Oluwafemi, O.S., Kalarikkal, N., Thomas, S. (Eds.), *Synthesis of Inorganic Nanomaterials*. Woodhead Publishing, pp. 121–139.
- Rattanachueskul, N., Saming, A., Kaowphong, S., Chumha, N., Chuenchom, L., 2017. Magnetic carbon composites with a hierarchical structure for adsorption of tetracycline, prepared from sugarcane bagasse via hydrothermal carbonization coupled with simple heat treatment process. *Bioresour. Technol.* 226, 164–172. <https://doi.org/10.1016/j.biortech.2016.12.024>.
- Rebekah, A., Bharath, G., Naushad, M., Viswanathan, C., Ponpandian, N., 2020. Magnetic graphene/chitosan nanocomposite: A promising nano-adsorbent for the removal of 2-naphthol from aqueous solution and their kinetic studies. *Int. J. Biol. Macromol.* 159, 530–538. <https://doi.org/10.1016/j.ijbiomac.2020.05.113>.
- Ren, X., Turcheniuk, K., Lewis, D., Fu, W., Magasinski, A., Zhang, M., Yushin, G., 2018. Conformal vapor deposition of iron phosphate onto carbon nanotubes for flexible high-rate cathodes. *Mater. Today Energy* 8, 143–150. <https://doi.org/10.1016/j.mtener.2018.04.002>.
- Sadeghfar, F., Ghaedi, M., Asfaram, A., Jannesar, R., Javadian, H., Pezeshkpour, V., 2018. Polyvinyl alcohol/Fe₃O₄@carbon nanotubes nanocomposite: Electrochemical-assisted synthesis, physicochemical characterization, optical properties, cytotoxicity effects

- and ultrasound-assisted treatment of aqueous based organic compound. *J. Ind. Eng. Chem.* 65, 349–362. <https://doi.org/10.1016/j.jiec.2018.05.006>.
- Sargazi, G., Afzali, D., Ebrahimi, A.K., Badoei-dalfard, A., Malek-abadi, S., Karami, Z., 2018. Ultrasound assisted reverse micelle efficient synthesis of new Ta-MOF@ Fe₃O₄ core/shell nanostructures as a novel candidate for lipase immobilization. *Mater. Sci. Eng., C* 93, 768–775. <https://doi.org/10.1016/j.msec.2018.08.041>.
- Sathya, A., Kalyani, S., Ranoo, S., Philip, J., 2017. One-step microwave-assisted synthesis of water-dispersible Fe₃O₄ magnetic nanoclusters for hyperthermia applications. *J. Magn. Magn. Mater.* 439, 107–113. <https://doi.org/10.1016/j.jmmm.2017.05.018>.
- Schleich, N., Danhier, F., Preat, V., 2014. Iron oxide-loaded nanotheranostics: Major obstacles to in vivo studies and clinical translation. *J. Control. Rel. Off. J. Control. Release Soc.* 198. <https://doi.org/10.1016/j.jconrel.2014.11.024>.
- Setyawan, H., Widiyastuti, W., 2019. Progress in the Preparation of Magnetite Nanoparticles through the Electrochemical Method. *Kona Powder Part. J.* 36, 145–155. <https://doi.org/10.14356/kona.2019011>.
- Shah, K.A., Tali, B.A., 2016. Synthesis of carbon nanotubes by catalytic chemical vapour deposition: A review on carbon sources, catalysts and substrates. *Mater. Sci. Semicond. Process.* 41, 67–82. <https://doi.org/10.1016/j.mssp.2015.08.013>.
- Sharifianjazi, F., Moradi, M., Parvin, N., Nemati, A., Jafari Rad, A., Sheysi, N., Abouchenari, A., Mohammadi, A., Karbasi, S., Ahmadi, Z., Esmailkhanian, A., Irani, M., Pakseresht, A., Sahmani, S., 2020. Shahedi Asl, Magnetic CoFe₂O₄ nanoparticles doped with metal ions: A review. *Ceram. Int.* 46, 18391–18412. <https://doi.org/10.1016/j.ceramint.2020.04.202>.
- Shi, Y., Xing, Y., Deng, S., Zhao, B., Fu, Y., Liu, Z., 2020. Synthesis of proanthocyanidins-functionalized Fe₃O₄ magnetic nanoparticles with high solubility for removal of heavy-metal ions. *Chem. Phys. Lett.* 753. <https://doi.org/10.1016/j.cplett.2020.137600> 137600.
- Siddiqui, M.T.H., Ahmed Baloch, H., Nizamuddin, S., Haris, M., Mubarak, N.M., Czajka, M., Khalid, M., Griffin, G.J., Srinivasan, M., 2020. Synthesis of novel magnetic carbon nano-composite from waste biomass: A comparative study of industrially adoptable hydro/solvothermal co-precipitation route, *Journal of Environmental. Chem. Eng.* 8. <https://doi.org/10.1016/j.jece.2019.103519> 103519.
- Simonazzi, A., Cid, A.G., Villegas, M., Romero, A.I., Palma, S.D., Bermúdez, J.M., 2018. Chapter 3 - Nanotechnology applications in drug controlled release. In: Grumezescu, A.M. (Ed.), *Drug Targeting and Stimuli Sensitive Drug Delivery Systems*. William Andrew Publishing, pp. 81–116.
- Singh, P., Upadhyay, C., 2018. Role of silver nanoshells on structural and magnetic behavior of Fe₃O₄ nanoparticles. *J. Magn. Magn. Mater.* 458, 39–47. <https://doi.org/10.1016/j.jmmm.2018.02.075>.
- Skomski, R., Sellmyer, D.J., 2006. Intrinsic and Extrinsic Properties of Advanced Magnetic Materials. In: Liu, Y., Sellmyer, D.J., Shindo, D. (Eds.), *Handbook of Advanced Magnetic Materials*. Springer, US, Boston, MA, pp. 1–57.
- Spiridonov, V.V., Panova, I., Afanasov, M.I., Zezin, S.B., Sybachin, A., Yaroslavov, A.A., 2018. Water-Soluble Magnetic Nanocomposites Based on Carboxymethyl Cellulose and Iron(III) Oxide. *Polym. Sci. - Series B* 60, 116–121. <https://doi.org/10.1134/S156009041801013X>.
- Starowicz, M., Starowicz, P., Zukrowski, J., Przewoźnik, J., Lemański, A., Kapusta, C., 2011. Electrochemical synthesis of magnetic iron oxide nanoparticles with controlled size. *J. Nanopart. Res. Interdiscip. Forum Nanoscale Sci. Technol.* 13, 7167–7176. <https://doi.org/10.1007/s11051-011-0631-5>.
- Sun, X., Zu, K., Liang, H., Sun, L., Zhang, L., Wang, C., Sharma, V. K., 2018. Electrochemical synthesis of ferrate(VI) using sponge iron anode and oxidative transformations of antibiotic and pesticide. *J. Hazard. Mater.* 344, 1155–1164. <https://doi.org/10.1016/j.jhazmat.2017.08.081>.
- Sundaraman, R.T.S., 2020. Synthesis and characterization of chicken eggshell powder coated magnetic nano adsorbent by an ultrasonic bath assisted co-precipitation for Cr(VI) removal from its aqueous mixture. *J. Environ. Chem. Eng.* <https://doi.org/10.1016/j.jece.2020.103877> 103877.
- Szabó, T., Bakandritsos, A., Tzitzios, V., Papp, S., Orösi, L., Galbaics, G., Musabekov, K., Bolatova, D., Petridis, D., Dekany, I., 2007. Magnetic iron oxide/clay composites: Effect of the layer silicate support on the microstructure and phase formation of magnetic nanoparticles. *Nanotechnology* 18, 285602–285609. <https://doi.org/10.1088/0957-4484/18/28/285602>.
- Tajyani, S., Babaei, A., 2018. A new sensing platform based on magnetic Fe₃O₄@NiO core/shell nanoparticles modified carbon paste electrode for simultaneous voltammetric determination of Quercetin and Tryptophan. *J. Electroanal. Chem.* 808, 50–58. <https://doi.org/10.1016/j.jelechem.2017.11.010>.
- Tartaj, P., González-Carreño, T., Serna, C., 2004. From Hollow to Dense Spheres: Control of Dipolar Interactions by Tailoring the Architecture in Colloidal Aggregates of Superparamagnetic Iron Oxide Nanocrystals. *Adv. Mater.* 16, 529–533. <https://doi.org/10.1002/adma.200305814>.
- Torabi, M., Sadrnezhad, S.K., 2010. Electrochemical synthesis of flake-like Fe/MWCNTs nanocomposite for hydrogen evolution reaction: Effect of the CNTs on dendrite growth of iron and its electrocatalytic activity. *Curr. Appl Phys.* 10, 72–76. <https://doi.org/10.1016/j.cap.2009.04.016>.
- Vangelista, S., Mantovan, R., Cocco, S., Lamperti, A., Salicio, O., Fanciulli, M., 2012. Chemical vapor deposition growth of Fe₃O₄ thin films and Fe/Fe₃O₄ bi-layers for their integration in magnetic tunnel junctions. *Thin Solid Films* 520, 4617–4621. <https://doi.org/10.1016/j.tsf.2011.10.128>.
- Veyret, R., Elaissari, A., Marianneau, P., Sall, A.A., Delair, T., 2005. Magnetic colloids for the generic capture of viruses. *Anal. Biochem.* 346, 59–68. <https://doi.org/10.1016/j.ab.2005.07.036>.
- Wang, J., Gao, M., Wang, D., Li, X., Dou, Y., Liu, Y., Pan, H., 2015. Chemical vapor deposition prepared bi-morphological carbon-coated Fe₃O₄ composites as anode materials for lithium-ion batteries. *J. Power Sources* 282, 257–264. <https://doi.org/10.1016/j.jpowsour.2015.02.058>.
- Wang, H., Liu, Y., Ifthikar, J., Shi, L., Khan, A., Chen, Z., Chen, Z., 2018. Towards a better understanding on mercury adsorption by magnetic bio-adsorbents with γ -Fe₂O₃ from pinewood sawdust derived hydrochar: Influence of atmosphere in heat treatment. *Bioresour. Technol.* 256, 269–276. <https://doi.org/10.1016/j.biortech.2018.02.019>.
- Wang, G., Zeng, Y., Zhou, F., Chen, X., Ma, Y., Zheng, L., Li, M., Sun, Y., Liu, X., Liu, H., Yu, R., 2020. One-step solvothermal synthesis of porous MnFe₂O₄ nanoflakes and their magnetorheological properties. *J. Alloy. Compd.* 819. <https://doi.org/10.1016/j.jallcom.2019.153044> 153044.
- Wang, P., Zhu, Y., Yang, X., Li, C., 2007. Electrochemical synthesis of magnetic nanoparticles within mesoporous silica microspheres. *Colloids Surf., A* 294, 287–291. <https://doi.org/10.1016/j.colsurfa.2006.08.015>.
- Xiang, W., Gebhardt, S., Gläser, R., Liu, C.-J., 2020. Millimeter-scale magnetic spherical metal-organic framework core-shell structured composites for recyclable catalytic applications. *Micropor. Mesopor. Mater.* 300. <https://doi.org/10.1016/j.micromeso.2020.110152> 110152.
- Yan, L., Li, S., Yu, H., Shan, R., Du, B., Liu, T., 2016. Facile solvothermal synthesis of Fe₃O₄/bentonite for efficient removal of heavy metals from aqueous solution. *Powder Technol.* 301, 632–640. <https://doi.org/10.1016/j.powtec.2016.06.051>.
- Yang, S., Xu, Y., Sun, Y., Zhang, G., Gao, D., 2012. Size-controlled synthesis, magnetic property, and photocatalytic property of uniform α -Fe₂O₃ nanoparticles via a facile additive-free hydrothermal route. *CrystEngComm* 14, 7915–7921. <https://doi.org/10.1039/C2CE25929J>.

- Yi, Y., Peng, Y., Xia, C., Wu, L., Ke, X., Nie, J., 2019. Influence of heat treatment on microstructures and magnetic properties of Fe-based soft magnetic composites prepared by co-precipitation method. *J. Magn. Magn. Mater.* 476, 100–105. <https://doi.org/10.1016/j.jmmm.2018.12.049>.
- Yu, C., Geng, J., Zhuang, Y., Zhao, J., Chu, L., Luo, X., Zhao, Y., Guo, Y., 2016. Preparation of the chitosan grafted poly (quaternary ammonium)/Fe₃O₄ nanoparticles and its adsorption performance for food yellow 3. *Carbohydr. Polym.* 152, 327–336. <https://doi.org/10.1016/j.carbpol.2016.06.114>.
- Yu, X., Tong, S., Ge, M., Zuo, J., Cao, C., Song, W., 2013. One-step synthesis of magnetic composites of cellulose@iron oxide nanoparticles for arsenic removal. *J. Mater. Chem. A* 1, 959–965. <https://doi.org/10.1039/C2TA00315E>.
- Yu, X., Shan, Y., Chen, K., 2018. Fabrication and characterization of morphology-tuned single-crystal monodisperse Fe₃O₄ nanocrystals. *Appl. Surf. Sci.* 439, 298–304. <https://doi.org/10.1016/j.apsusc.2017.12.229>.
- Zeng, X., Zhu, L., Yang, B., Yu, R., 2020. Necklace-like Fe₃O₄ nanoparticle beads on carbon nanotube threads for microwave absorption and supercapacitors. *Mater. Des.* 189, <https://doi.org/10.1016/j.matdes.2020.108517> 108517.
- Zhan, Y., Long, Z., Wan, X., Zhang, J., He, S., He, Y., 2018. 3D carbon fiber mats/nano-Fe₃O₄ hybrid material with high electromagnetic shielding performance. *Appl. Surf. Sci.* 444, 710–720. <https://doi.org/10.1016/j.apsusc.2018.03.006>.
- Zhang, Y., Dong, Y., Zhou, B., Chi, Q., Chang, L., Gong, M., Huang, J., Pan, Y., He, A., Li, J., Wang, X., 2020. Poly-paraxylene enhanced Fe-based amorphous powder cores with improved soft magnetic properties via chemical vapor deposition. *Mater. Des.* 191, <https://doi.org/10.1016/j.matdes.2020.108650> 108650.
- Zhang, M., Jia, J., Huang, K., Hou, X., Zheng, C., 2018. Facile electrochemical synthesis of nano iron porous coordination polymer using scrap iron for simultaneous and cost-effective removal of organic and inorganic arsenic. *Chin. Chem. Lett.* 29, 456–460. <https://doi.org/10.1016/j.ccllet.2017.09.062>.
- Zhang, H.-J., Liu, L.-Z., Zhang, X.-R., Zhang, S., Meng, F.-N., 2019. Microwave-assisted solvothermal synthesis of shape-controlled CoFe₂O₄ nanoparticles for acetone sensor. *J. Alloy. Compd.* 788, 1103–1112. <https://doi.org/10.1016/j.jallcom.2019.03.009>.
- Zhang, B.-T., Wang, Q., Zhang, Y., Teng, Y., Fan, M., 2020. Degradation of ibuprofen in the carbon dots/Fe₃O₄@carbon sphere pomegranate-like composites activated persulfate system. *Sep. Purif. Technol.* 242, <https://doi.org/10.1016/j.seppur.2020.116820> 116820.
- Zhao, Z., Zhang, X., Zhou, H., Liu, G., Kong, M., Wang, G., 2017. Microwave-assisted synthesis of magnetic Fe₃O₄-mesoporous magnesium silicate core-shell composites for the removal of heavy metal ions. *Micropor. Mesopor. Mater.* 242, 50–58. <https://doi.org/10.1016/j.micromeso.2017.01.006>.
- Zhou, G., Wang, Y., Zhou, R., Wang, C., Jin, Y., Qiu, J., Hua, C., Cao, Y., 2019. Synthesis of amino-functionalized bentonite/CoFe₂O₄@MnO₂ magnetic recoverable nanoparticles for aqueous Cd²⁺ removal. *Sci. Total Environ.* 682, 505–513. <https://doi.org/10.1016/j.scitotenv.2019.05.218>.